

Combined NO_x and SO_x Removal in Pressurized CO₂ Treatment Processes

Modeling and Evaluation of CO₂ Conditioning Systems for CCS Purposes

Master's Thesis in Sustainable Energy Systems

IVAR KWANT

DEPARTMENT OF SPACE, EARTH AND ENVIRONMENT

CHALMERS UNIVERSITY OF TECHNOLOGY
Gothenburg, Sweden 2025
www.chalmers.se

MASTER'S THESIS 2025

**Combined NO_x and SO_x Removal in Pressurized
CO₂ Treatment Processes**

Modeling and Evaluation of CO₂ Conditioning Systems for
CCS Purposes

IVAR KWANT



CHALMERS
UNIVERSITY OF TECHNOLOGY

Department of Space, Earth and Environment

Division of Energy Technology

High Temperature Processes group

CHALMERS UNIVERSITY OF TECHNOLOGY

Göteborg, Sweden 2025

Combined NO_x and SO_x Removal in Pressurized CO₂ Treatment Processes
Modeling and Evaluation of CO₂ Conditioning Systems for CCS Purposes
IVAR KWANT

© IVAR KWANT, 2025.

Supervisor: Jakob Johansson, Department of Space, Earth and Environment

Examiner: Professor Fredrik Normann, Department of Space, Earth and Environment

Master's Thesis 2025

Department of Space, Earth and Environment

Division of Energy Technology

High Temperature Processes group

Chalmers University of Technology

SE-412 96 Göteborg

Telephone +46 31 772 1000

Cover: Flowsheet of sour compression process in Aspen Plus®.

Typeset in L^AT_EX

Printed by Chalmers Reproservice

Göteborg, Sweden 2025

Abstract

Today's extensive use of thermal conversion processes is a double-edged sword that brings economic prosperity but at the cost of rapid climate change. Carbon capture, utilization or storage technologies mitigate CO₂ emissions and decouple the effects of thermal conversion processes in terms of climate change.

The captured CO₂ must meet purity requirements with regards to contaminants for downstream transport, storage, as well as utilization processes. Nitrogen and sulfur oxides (NO_x and SO_x) are common contaminants from thermal conversion. During compression, NO_x and SO_x form acids, which may corrode equipment if left uncontrolled. However, a sour compression process for combined NO_x and SO_x removal could treat the CO₂ by absorbing the formed acids.

A numerical model of a sour compression process is constructed and applied to a CO₂ compression train to investigate the possibilities of reaching required CO₂ specifications. It was found that sustained time at elevated pressures is a viable way of oxidizing NO to NO₂, but only in the presence of oxygen. However, the oxidation of NO is the bottleneck in the process to reach the CO₂ quality specifications as NO₂ and SO₂ are both absorbed with high efficiency. The high pressure and CO₂ content of the incoming gas caused a significant accumulation of carbonates, the solubility of which is strongly related to pH. This is important to consider due to precipitation concerns and CO₂ loss, among other things.

Keywords: Carbon capture and storage, CCS, NO_x, SO_x, process modeling, sour compression, pressurized absorption.

Acknowledgements

First and foremost, I would like to extend a warm thank you to my thesis supervisor, Jakob Johansson, for giving me the opportunity to take on this task. Your expertise has been invaluable for this thesis, and your help greatly appreciated. I would also like to thank my examiner, Professor Fredrik Normann. Your valuable insights and constructive advice has given this thesis that little extra in terms of precision and clarity. Thank you also to Rosa Citra Aprilia, for going out of your way to help me get up and running at the beginning of this project even though it was not expected of you, and to Judit Fortet Casabella and Aaron Qiyu Liu for all the help with installing the software.

Ivar Kwant, Göteborg, June 2025

List of Acronyms

Below is the list of acronyms that have been used throughout this thesis, in alphabetical order:

AFOLU	Agriculture, Forestry and Other Land Use
BECCS	Bioenergy with Carbon Capture and Storage
CCS	Carbon Capture and Storage
CCUS	Carbon Capture, Utilization and Storage
CLC	Chemical Looping Combustion
EBN	Energie Beheer Nederland
EOR	Enhanced Oil Recovery
EU	European Union
GHG	Greenhouse Gases
IPCC	Intergovernmental Panel on Climate Change
MEA	Monoethanolamine
NO _x	Nitrous oxides
PCI	Project of Common Interest
SO _x	Sulfur oxides
UN	United Nations

Nomenclature

Below is the nomenclature of parameters that have been used throughout this thesis.

Parameters

R	Liquid to gas mass ratio
\dot{L}	Liquid mass flow (kg/s)
\dot{G}	Gas mass flow (kg/s)
$C_{S(VI)}$	S(VI) concentration (g/L)
C_{CO_3}	CO ₃ concentration (g/L)
\dot{m}	Mass flow (kg/h)
\dot{Q}	Volumetric flow (m ³ /h)
τ	Residence time (s)
l	Length (m)
d	Diameter (m)
h	Height (m)
ε	Packing material void fraction

Contents

List of Acronyms	ix
Nomenclature	xi
List of Figures	xv
List of Tables	xvii
1 Introduction	1
2 Aim	3
2.1 Scope	3
3 Theory	5
3.1 Carbon Capture and Storage (CCS)	5
3.1.1 Post-combustion Capture (Amine Based Absorption)	5
3.1.2 Oxyfuel Combustion	6
3.1.3 Chemical Looping Combustion (CLC)	7
3.1.4 CO ₂ Transport and Storage	8
3.1.5 Carbon Capture, Utilization and Storage (CCUS)	10
3.1.6 Bioenergy with Carbon Capture and Storage (BECCS)	10
3.2 CO ₂ Contaminants and Their Associated Problems	11
3.3 Combined NO _x and SO _x removal	12
3.3.1 NO _x chemistry	13
3.3.2 Absorption Chemistry of Combined NO _x and SO _x removal	13
4 Method	15
4.1 Model Description	16

4.1.1	Properties Setup	16
4.1.2	Flowsheet and Simulation	17
4.2	Design Parameter Study	22
4.2.1	NO Oxidation	22
4.2.2	Absorption Column	24
5	Results	25
5.1	Parameter Study	27
5.1.1	NO Oxidation	28
5.1.2	Absorption Column	32
6	Discussion	37
6.1	Parameter Study	37
6.1.1	NO Oxidation	38
6.1.2	NO _x and SO _x Absorption	39
6.2	Aftertreatment of Outgoing Gas	40
6.3	Areas of Uncertainty	40
6.3.1	Pressurized Absorption Processes	40
6.3.2	Validity of Chemical Model	41
6.4	Areas of Further Study	41
6.4.1	Experimental Trials	41
6.4.2	Study of Impact of Sulfur Content	42
6.4.3	Modeling of Alternative Process Configurations	42
6.4.4	Process Optimization and Economic Analysis	42
7	Conclusion	43
	Bibliography	45

List of Figures

3.1	Schematic overview of a general amine based absorption process.	6
3.2	Schematic overview of oxyfuel combustion.	7
3.3	Schematic overview of CLC.	8
3.4	Different global warming pathways, according to IPCC [28].	11
3.5	Simplified visual representation of NO _x and SO _x co-removal reaction mechanism.	14
4.1	Visual representation of the method used for this thesis.	15
4.2	Flowsheet of sour compression process in Aspen Plus®.	18
5.1	Graph of NO content across the process at varying oxygen levels in %, for post-combustion gas.	28
5.2	Graph of NO content depending on discharge pressure of the second compressor, for post-combustion gas (0.1% O ₂).	28
5.3	Graph of NO content depending on discharge pressure of the second compressor, for oxyfuel gas (5.5% O ₂).	29
5.4	Graph of NO content depending on discharge pressure of the second compressor, for CLC gas (1.1% O ₂).	29
5.5	Graph of NO content depending on residence time in the first intercooler, for post-combustion gas.	30
5.6	Graph of NO content depending on residence time in the first intercooler, for oxyfuel gas.	30
5.7	Graph of NO content depending on residence time in the first intercooler, for CLC gas.	31
5.8	Graph of NO content depending on residence time in the second intercooler, for post-combustion gas.	31

5.9	Graph of NO content depending on residence time in the second intercooler, for oxyfuel gas.	32
5.10	Graph of NO content depending on residence time in the second intercooler, for CLC gas.	32
5.11	Graph of NO content depending on column height, for oxyfuel gas.	33
5.12	Graph of NO content depending on absorber pH, for oxyfuel gas.	34
5.13	Graph of absorbent liquid carbonate content at varying pH, for oxyfuel gas. . .	34
5.14	Graph of NO content depending on absorber R , for oxyfuel gas.	35

List of Tables

3.1	Specifications for CO ₂ quality, values in ppm-mol unless otherwise specified.	10
4.1	Chemical components of the system, as added in Aspen Plus®.	16
4.2	Global reactions of the system, as specified in Aspen Plus®.	17
4.3	Gas-phase reaction of the system, as specified in Aspen Plus®.	18
4.4	Proposed reaction mechanism for combined NO _x and SO _x removal [9].	19
4.5	Absorption column internals settings.	19
4.6	Ingoing gas composition, in volume fractions.	21
4.7	Summary of the most important design parameters for the model.	22
5.1	Summary of important resulting parameters.	25
5.2	NO flows and oxidation results for the process models.	25
5.3	Outgoing gas composition for process models, in mol-ppm unless otherwise specified, with specifications used for reference.	26
5.4	Concentration of accumulated species in bleed water (g/L). * Released upon pressure decrease.	27
5.5	CO ₂ losses from the system.	27
5.6	Tube lengths and their corresponding residence times.	30
5.7	Column heights and their corresponding residence times.	33
5.8	Investigated split fractions, resulting <i>R</i> , and associated column diameters.	35

1

Introduction

Thermal conversion processes such as combustion are a cornerstone for maintaining our way of life and standard of living. The industrial revolution, fueled mostly by coal, laid the foundation for today's strong western economies [1], and fossil fuel use is still heavily linked to economic growth and increased prosperity for societies using them [2]. At the same time, emissions associated with the use of fossil fuels also pose a grave threat to the environment, as higher atmospheric CO₂ concentrations cause rapid climate change [3]. The United Nations (UN) sustainable development goal 13, regarding climate action, states that global warming needs to be limited to 1.5 °C compared to pre-industrial levels to limit the severe effects of climate change [4]. To take part in achieving this goal, the European Union (EU) has made commitments to lower its emissions of greenhouse gases (GHG) through the European Green Deal. The main objective is to become the first climate neutral continent by 2050, with the milestone of achieving a 55% reduction of GHG emissions by 2030 as compared to 1990 [5]. One of Sweden's own climate goals is to have net zero GHG emissions by 2045 [6], which is in line with the EU's targets. Carbon capture and storage (CCS) as well as carbon capture, utilization and storage (CCUS) have been deemed essential technologies for achieving these aims going forward [7].

CCS involves the capture of CO₂ from point sources, i.e. industrial sites where large quantities of CO₂ are generated. This CO₂ can be stored underground, or utilized as a feedstock for other purposes. An important step in CCS is the compression of the captured CO₂ to facilitate transport and end storage. In this step, it is common for contaminants in the CO₂ stream, namely nitrogen and sulfur oxides (NO_x and SO_x), to form acids, causing corrosion and eventually equipment failure [8]. This poses a significant challenge for mainstream CCS adoption, as the continuous need for maintenance makes the process unreliable and economically unsustainable. CO₂ purity specifications for transport hubs and storage sites are therefore becoming increasingly stringent and hard to meet with today's conventional flue gas cleaning technologies.

To address this need for increasingly pure CO₂ streams, an effective method of further cleaning these from NO_x and SO_x is needed to reach stricter impurity tolerances. One such method is using a pressurized system for combined NO_x and SO_x removal. The increased pressure influences the mass transfer of NO_x and SO_x and promotes the formation of reaction species that are water soluble. Hence, they can be absorbed with wet scrubbing systems, cleaning the CO₂ stream [9]. However, there are differing requirements on purity depending on transport method, as well as end storage location or area of use. Additionally, the conditions of the incoming CO₂ stream may vary depending on the capture method, fuel composition, and type of industry. It is unknown what is required from the CO₂ conditioning process to meet the purity specifications for these different cases. This thesis will seek to evaluate if these specifications can be met for different sources of emission, and the process requirements in doing so.

2

Aim

The aim of this thesis is to model and evaluate pressurized CO₂ conditioning processes in which NO_x and SO_x are removed. This is to prevent them from undergoing reactions forming acids, in turn minimizing wear on CCS equipment and ensuring its reliable operation. It will be investigated whether pressurized CO₂ cleaning systems can condition the CO₂ to meet quality specifications for transport, storage, and utilization with satisfactory results for CO₂ streams from different capture methods, namely post-combustion capture, oxyfuel combustion and chemical looping combustion (CLC). Ideally this will contribute towards making CCS more economically viable, which would increase its appeal for commercial use. This is of importance since CCS has been identified as an important contributing factor in reaching climate targets [7].

2.1 Scope

The model itself will be representative of the pressurized absorption process in which contaminants, such as SO_x and NO_x, are removed from captured CO₂. In the case of post-combustion, this means that the main step in the CCS process, i.e. the primary separation of CO₂ from the other species in the flue gas, has already taken place. Exhaust streams obtained by other means than post-combustion will also be investigated. In this case no prior separation stages will be accounted for. Furthermore, the transport and end storage of the CO₂ will not be within the scope of this thesis, and will thus not be accounted for in the model. However, it is worthy of notice that the specifications of the CO₂ stream are also set in accordance with the requirements of these steps. Additionally, there are many areas in which captured CO₂ can be utilized, as per Section 3.1.5. This thesis has provided general results which can be used for reference broadly in this context.

3

Theory

3.1 Carbon Capture and Storage (CCS)

Carbon Capture and Storage (CCS) is a technology in which CO₂ is captured from large industrial exhaust sites and separated from the other contents of the exhaust gases, after which it is compressed to reduce its volume for transport. It is possible to transport CO₂ by, for example, transferring it to pressure vessels, or by ship or pipeline to its end storage location. Commonly, these locations are geological formations underground, such as porous rock [10]. The CO₂ can also be utilized for other purposes, which is explained further in Section 3.1.5.

3.1.1 Post-combustion Capture (Amine Based Absorption)

There are several technologies for separating CO₂ from the other contents of the flue gases. Despite CCS as a whole not being a widely adopted technology, absorption with aqueous amines is the most common method of CO₂ capture in use. Monoethanolamine (MEA) is the most commonly used solvent for this purpose, but there are alternatives [11]. The process may vary somewhat depending on the conditions and contents of the flue gas, but a typical process could be explained as per this section. First, the flue gases are sent through a blower to raise the pressure. Some type of contaminant removal unit (e.g. a scrubber) is then used to remove for example SO_x and heavy metals, as the amine solvents are sensitive to these. The flue gases are then cooled to approximately 40°C, as this is thermodynamically favorable for the absorption process. After this, the cooled flue gases are fed to the absorption column, where they are met with the amine solution which absorbs $\geq 90\%$ of CO₂. The flue gases subjected to this absorption stage are then led out to the atmosphere at the top of the column. The solvent is regenerated in a so-called stripper column, where the mixture is heated, separating the CO₂ through vaporization. Afterwards the CO₂ is compressed for ease of transport, and dehydrated,

as some water is still left [12]. A visual representation of a general post-combustion process is shown in Figure 3.1.

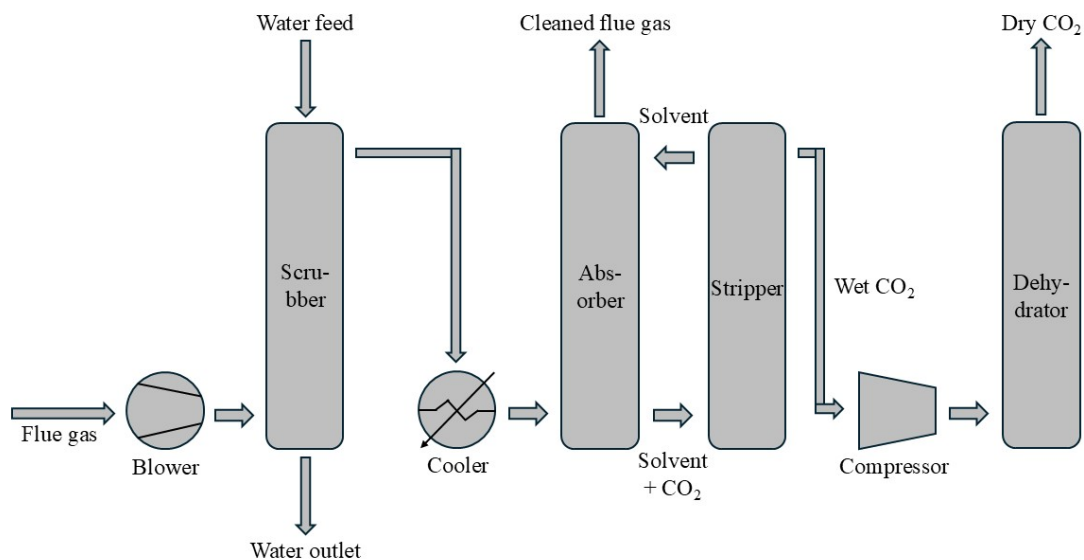


Figure 3.1: Schematic overview of a general amine based absorption process.

3.1.2 Oxyfuel Combustion

Oxyfuel Combustion is a technology in which fuel is burnt in a oxygen-enriched environment instead of ambient air. Oxygen is separated from air, so that the large quantities of nitrogen in air do not enter the combustion chamber. The oxygen is then supplied to the reactor, together with some recycled flue gases to control the temperature. This gives an exhaust gas that consists mainly of the combustion products CO₂ and water, where the water can be separated through condensation [13]. This results in a concentrated stream of CO₂ which can be captured. A visual representation of an oxyfuel combustion process is shown in Figure 3.2.

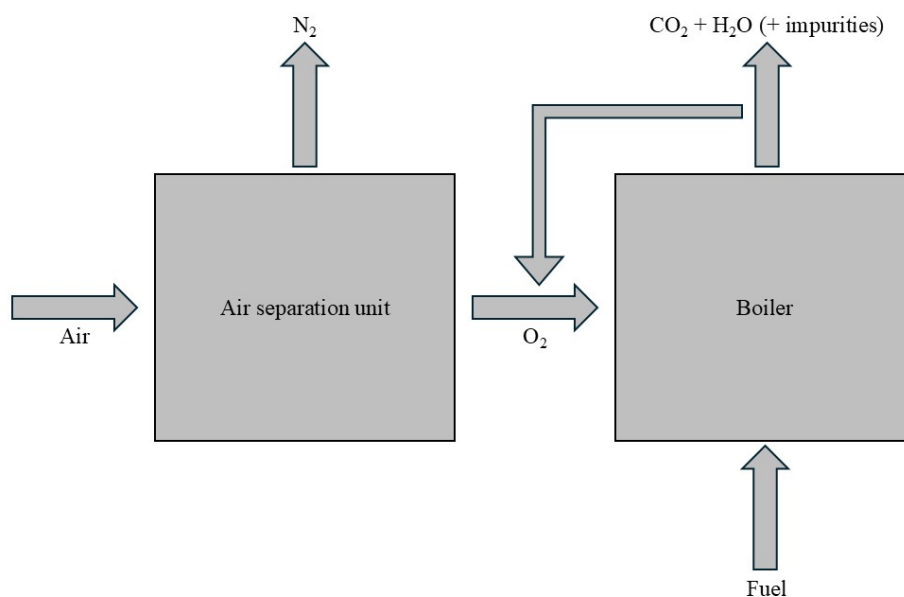


Figure 3.2: Schematic overview of oxyfuel combustion.

3.1.3 Chemical Looping Combustion (CLC)

Chemical Looping Combustion (CLC) is a technology where two interlinked fluidized bed reactors are used. One reactor is the so-called air reactor, and one is the fuel reactor. Air is supplied to the air reactor, where it comes into contact with the bed material. As opposed to normal fluidized bed reactors which mainly use sand, the bed material consists of a metal oxide which acts as an oxygen carrier. This metal oxide undergoes oxidation in the air reactor, and the oxygen from the air is bound to the metal oxide. The other contents of the air, i.e. mostly nitrogen gas, is led out of the air reactor and is therefore not present when combustion takes place. The now oxidized mineral is then transported to the fuel reactor. There, the oxygen is released as the metal oxide is reduced. The fuel is supplied to the fuel reactor where it is combusted, forming CO₂ and water. The water can be separated through condensation, giving a concentrated CO₂ stream [14]. A visual representation of a CLC process is shown in Figure 3.3.

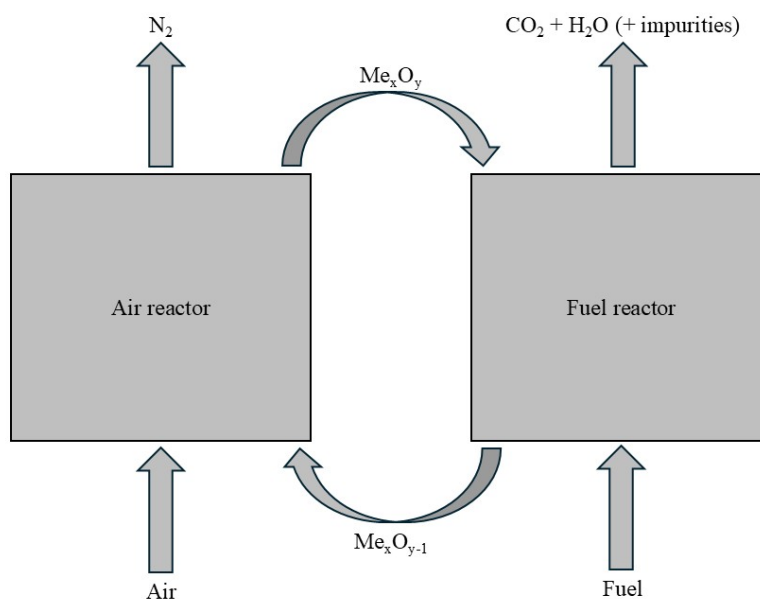


Figure 3.3: Schematic overview of CLC.

3.1.4 CO_2 Transport and Storage

The CO_2 has to be transported one way or another to its end storage location. The most common method is pipeline transport, which sees frequent use today [15]. CO_2 can be transported through pipeline in several different states: gas, liquid or supercritical (critical point at 73.8 bar, 304.25 K). Supercritical condition is the most common because of the high density and low viscosity of CO_2 in this state, which makes the transport more efficient [16]. For smaller quantities and distances, it is not uncommon to transport by truck or rail [15]. These methods can be used to transport liquid CO_2 to end storage locations where pipelines are not available, or to CO_2 hubs from where they can be handled further. Ships can also be used for these purposes, but for offshore applications [17]. The CO_2 is then injected into geological formations underground, such as depleted oil and gas fields, saline aquifers and porous rock. It can also be injected into operational oil fields in a process called enhanced oil recovery (EOR). When CO_2 mixes with the crude oil, the crude oil's pressure increases and its viscosity decreases, which aids in increasing the production from the field [18]. As more crude oil is extracted, there is no real environmental benefit to utilizing EOR, even though it means CO_2 is stored underground.

There are ongoing CCS projects which are of relevance to this thesis in particular, as their purity specifications have been used for reference when judging results. One such example is the Aramis transport hub in Rotterdam, the Netherlands. This project is a collaboration between privately-owned Shell and TotalEnergies, as well as Energie Beheer Nederland (EBN) and Gasunie, owned by the Dutch state. The project seeks to offer a solution for lowering CO₂ emissions for hard-to-abate industries in western Europe, and has been designated as a Project of Common Interest (PCI) by the EU, as well as declared a project of national importance by the Dutch state. CO₂ is captured locally at industrial sites, and is then transported either by ship or pipeline to Aramis' collection hub in the Rotterdam harbor, where it is compressed. The CO₂ is then sent via pipeline to an offshore distribution platform in the North Sea. From there the CO₂ is distributed to several smaller injection platforms, and stored underground in depleted natural gas fields. An open-access principle is followed, meaning that new CO₂ suppliers and storage facilities can be connected continuously. The capacity is up to 22 Mton CO₂ per year [19]. For reference, the Netherlands emitted 144 Mton CO₂-equivalents in 2024 [20]. The CO₂ purity specifications as used in this thesis have been set so as to limit the corrosive effects on the project infrastructure [21].

Another CCS project is the Northern Lights project in Bergen, Norway: a joint venture between Shell, TotalEnergies and state-owned corporation Equinor. Similarly to Aramis, Northern Lights is an open source transport and storage site, offering a solution for industrial actors seeking to lower their CO₂ emissions to the atmosphere. The receiving terminal is constructed for liquid CO₂ transported by ship. From there, the CO₂ is transported by pipeline and injected underground into saline aquifers off the Norwegian coast [22]. The specifications are mainly set with the intention of limiting the occurrence of corrosive fluids, which might otherwise bring safety and structural integrity concerns. Furthermore, the specifications seek to cater to as wide a range of emission sources as possible to allow for more actors to abate their emissions [23]. The capacity will be a minimum of 5 Mton CO₂ per year [22], in relation to Norway's total GHG emissions of 47 Mton CO₂-equivalents in 2023 [24]. Specifications for acceptable CO₂ quality for both the Aramis and Northern Lights projects are shown in Table 3.1. These specifications were used for reference when judging simulation results.

Table 3.1: Specifications for CO₂ quality, values in ppm-mol unless otherwise specified.

Specie	Aramis [21]	Northern Lights [25]
CO ₂ (minimum, mol%)	≥ 95	≥ 99.81
O ₂	≤ 10	≤ 10
N ₂	≤ 2.4 (mol%)	≤ 50
NO _x	≤ 1.5	≤ 1.5
SO _x	≤ 10	≤ 10
H ₂ O	≤ 30	≤ 30

3.1.5 Carbon Capture, Utilization and Storage (CCUS)

Carbon Capture, Utilization and Storage (CCUS) follows the same principles as CCS, but instead of being stored underground, the CO₂ is viewed as a feedstock for other purposes. Captured CO₂ can have many uses for different industries depending on the process it is subjected to, which contributes to more efficient use of resources and stimulates a circular economy. Utilization options for captured CO₂ include, but are not limited to, production of chemicals (such as methanol or urea), polymers, pharmaceuticals, nanomaterials, and uses within the food and beverage industry [26].

3.1.6 Bioenergy with Carbon Capture and Storage (BECCS)

Bioenergy with Carbon Capture and Storage (BECCS) is a technique that uses biomass as fuel, capturing and storing the resulting CO₂ emissions through CCS. Since biomass absorbs CO₂ during growth, which is then not released after combustion, BECCS offers the potential for net-negative emissions [27]. Figure 3.4 shows the importance of CO₂ emission reduction within the fossil fuel and industry sector, Agriculture, Forestry, and Other Land Use (AFOLU) sector, as well as through BECCS, for some different global warming pathways, according to the models of the Intergovernmental Panel on Climate Change (IPCC). For these pathways global warming is limited to the 1.5 °C target with no or limited overshoot. P1 represents an optimistic case where future innovations lower energy demand, while standards of living rise. P2 represents a case with a broad societal sustainability focus in terms of, for example, energy intensity, human development, and consumption patterns. In P3, societal and technological development follow historical patterns with only lesser changes in consumption, while GHG-intensive lifestyles

become the norm worldwide in P4. BECCS is clearly important in most scenarios, particularly where compromises in standards of living are avoided.

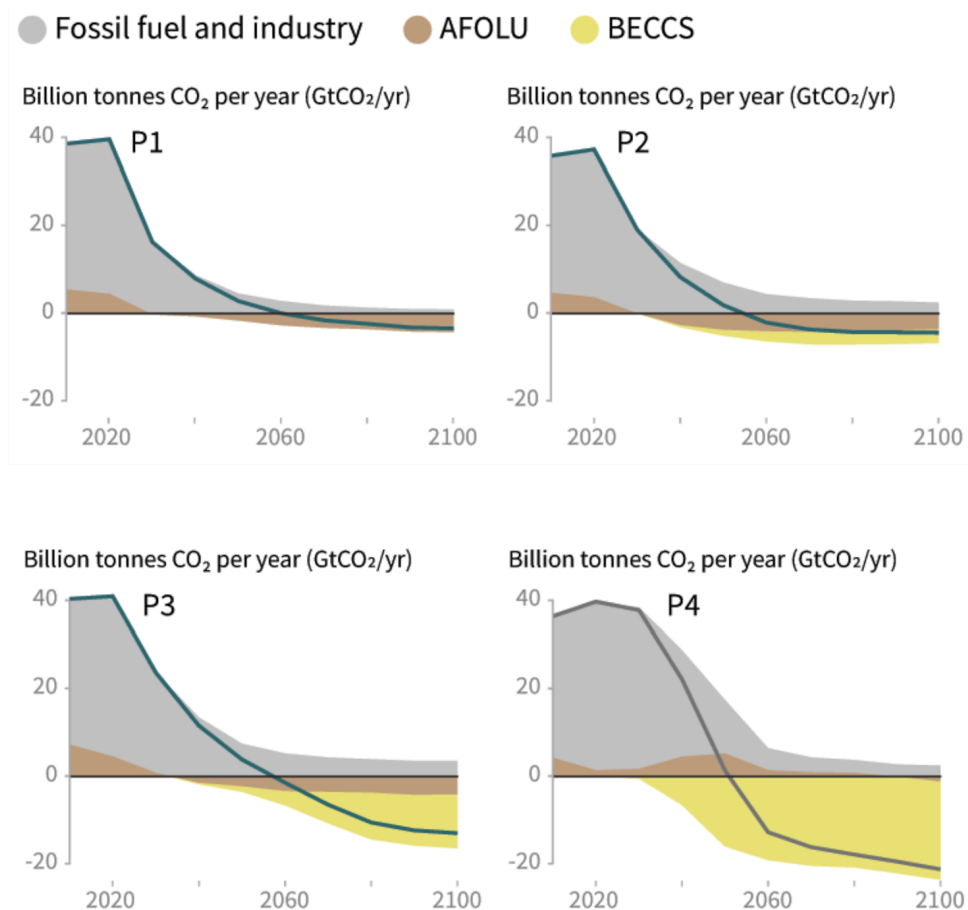
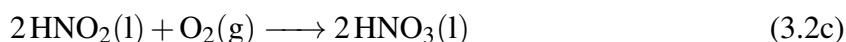
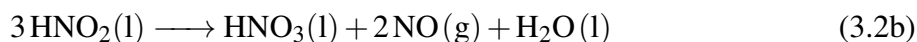
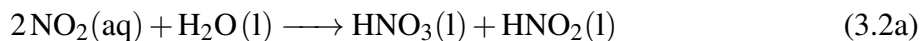


Figure 3.4: Different global warming pathways, according to IPCC [28].

3.2 CO₂ Contaminants and Their Associated Problems

When CO₂ is captured, so are smaller amounts of undesired compounds such as NO_x and SO_x. Under the high pressures associated with CO₂ compression, NO_x and SO_x react and form strong acids, namely sulfuric acid (H₂SO₄) and nitric acid (HNO₃). NO₂ is of particular importance since the reactions forming H₂SO₄ and HNO₃ do not occur in its absence [29]. The proposed global reaction for the formation of H₂SO₄ under CO₂ transport conditions is shown in Equation 3.1, and the formation route for HNO₃ in Equations 3.2a-3.2c [30].



The primary issue with these acids is their corrosive effect on metals commonly used in equipment used for CO₂ transport and storage, such as carbon steel. Carbon steel is, to a large extent, used in CO₂ pipelines due to it being a readily available material with relatively low cost and high strength [31]. The corrosion from H₂SO₄ and HNO₃ exposure may therefore affect the structural integrity of these pipelines negatively over time, as carbon steel is more susceptible to corrosion than for example stainless steel. However, higher alloy steels used in for example injection equipment have also shown susceptibility to corrosion, albeit at a lower rate [32]. Furthermore, the formation of solid corrosion byproducts such as FeSO₄ and elemental sulfur can cause clogging [29]. This can be an issue particularly when CO₂ is injected into reservoirs, as the solids can clog both the injection point as well as passages in the reservoir itself [31].

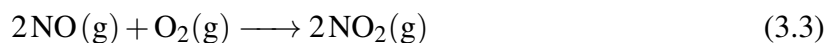
The cleaning processes discussed in this thesis take place after CO₂ capture. However, NO_x can cause problems in post-combustion capture processes in themselves as well. NO_x can react with MEA, degrading it to other amines. In the addition to lessening the efficiency of the process in itself, these amines can have potential negative health and environmental effects [33]. More effective NO_x removal before the CO₂ absorption would thus be beneficial also, and similar absorption principles to the one covered by this thesis could be of interest for this application.

3.3 Combined NO_x and SO_x removal

An integral part of this thesis work is the removal process upon which it is based. This process, as well as the associated chemistry, will be explained in more detail in this section.

3.3.1 NO_x chemistry

NO_x is formed in most combustion reactions, which is an important issue because of its impact as a pollutant in the atmosphere. There are two main ways of NO_x formation: fuel NO_x and thermal NO_x. Fuel NO_x is the result of nitrogen bound to the fuel undergoing reactions in the combustion process. Thermal NO_x on the other hand is formed from nitrogen in the air, a process which is dependent on temperature, and dominant at temperatures above 1300 °C [34]. This makes thermal NO_x the prevalent route of NO_x formation for thermal conversion processes using homogeneous fuels with high energy contents, such as for example coal combustion. On the other hand, heterogeneous fuels such as biomass or household waste have lower energy contents and higher moisture contents, which makes the combustion temperature lower. However these fuels contain more chemically bound nitrogen, leading to fuel NO_x formation. The two most relevant species of NO_x, NO and NO₂, are in thermodynamic equilibrium. At the temperatures of most combustion reactions the formation of NO is favored. This is an issue for the removal of NO_x from the flue gases through absorption, since NO is much less soluble than NO₂ in water, which is commonly used as a solvent for flue gas treatment systems. Thus, it is desired to allow for NO₂ to be formed instead [9]. This oxidation occurs spontaneously, however at timescales that are unreasonable to account for in flue gas cleaning processes (tens of minutes to hours). This can be remedied by introducing oxidation chemicals, such as ClO₂, O₃ or H₂O₂, which oxidize NO to NO₂ [35]. This requires purchasing in bulk or production on-site as well as the possible need for handling of byproducts, all of which are associated with additional costs. Alternatively, it is possible to pressurize the system, which causes the partial pressure of NO and O₂ to increase leading to an increased rate of oxidation of NO to NO₂ [9]. The oxidation reaction of NO to NO₂ is shown in Equation 3.3.



3.3.2 Absorption Chemistry of Combined NO_x and SO_x removal

The absorption process for flue gas cleaning aims to remove NO₂, and SO₂ if present. This is only the case if sulfur is present in the fuel, which it often is in the case of fossil fuels such as coal. The presence of sulfite, S(IV), which is formed from absorbed SO₂, is vital in the absorbent liquid stream for the absorption of NO₂, as it plays an integral role in the co-removal

reaction mechanism [35]. If not present through the gas itself, S(IV) can be added to the liquid absorbent to facilitate the reactions for NO_x removal. SO_2 forms an equilibrium with SO_3^{2-} , which in turn is in equilibrium with HSO_3^- . Together, SO_3^{2-} and HSO_3^- are the two S(IV) species. S(IV) reduces $\text{NO}_2(\text{aq})$ to NO_2^- , forming SO_4^{2-} , S(VI), in the process. This reaction is fast, and as mentioned, key for NO_2 absorption as SO_4^{2-} and NO_2^- are formed. These are water-soluble compounds and can therefore be removed with the water stream after wet scrubbing has occurred. Note that this is a reduced reaction mechanism comprised of the rate limiting reactions of the full reaction mechanism [9]. A visual representation of the NO_x and SO_x co-removal reaction mechanism can be seen in Figure 3.5.

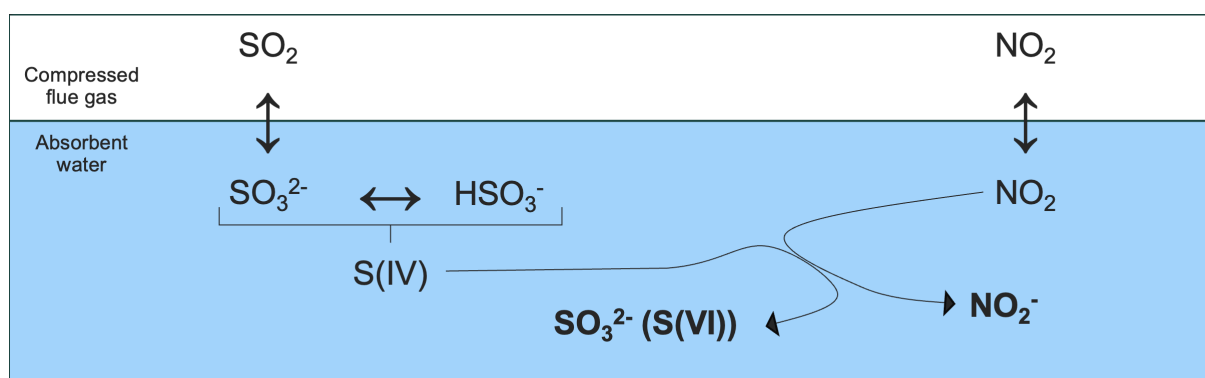
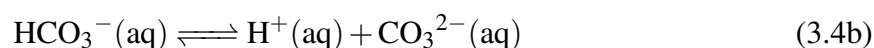


Figure 3.5: Simplified visual representation of NO_x and SO_x co-removal reaction mechanism.

Carbonate chemistry was also found to be important for this thesis. CO_2 forms an equilibrium with water according to the reaction in Equation 3.4a. According to Henry's law, which states that the solubility of a gas in a liquid is proportional to the partial pressure of the gas above the liquid [36], more CO_2 is dissolved in water as its partial pressure increases, in this case by raising the pressure of the considered process. Consequently, more carbonates are formed, as per the equilibria in Equations 3.4a-3.4b.



4

Method

A software model of the flue gas cleaning process was constructed, which was used to run simulations with different inlet gas compositions from different CO₂ capture methods: post-combustion capture, oxyfuel combustion and CLC. The importance of a selection of parameters pertaining to the compression stage as well as the absorption column were investigated in a design parameter study. One parameter was studied at a time, and the model was simulated for a range of values of the parameter in question. The results of the simulations were either judged in terms of NO oxidation, or in terms of NO₂ and SO₂ absorption as well as CO₂ loss. The learnings of the parameter study were applied to the model continuously so as to obtain as ideal a process as possible. A visual representation of the method can be seen in Figure 4.1.

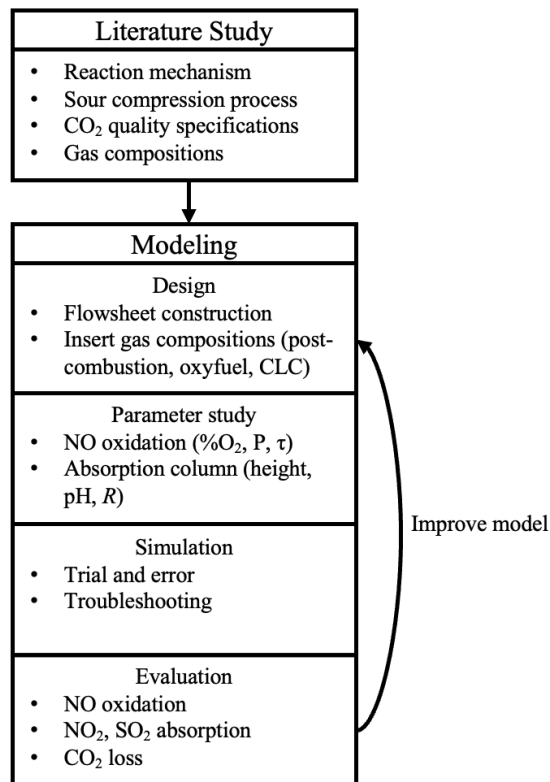


Figure 4.1: Visual representation of the method used for this thesis.

4.1 Model Description

Aspen Plus[®] V14 was used to model the NO_x and SO_x removal process. The following section will explain the setup of the model.

4.1.1 Properties Setup

Table 4.1: Chemical components of the system, as added in Aspen Plus[®].

Component ID/Alias	Component Name
NO ₂	Nitrogen Dioxide
O ₂ S	Sulfur Dioxide
N ₂	Nitrogen
H ₂ O	Water
HNO ₂	Nitrous Acid
HNO ₃	Nitric Acid
HSO ₃ ⁻	Hydrogen Sulfite
SO ₃ ²⁻	Sulfite
NO ₂ ⁻	Nitrite
NO ₃ ⁻	Nitrate
H ⁺	Hydrogen Ion
H ₂ SO ₄	Sulfuric Acid
N ₂ O	Nitrous Oxide
HSO ₄ ⁻	Hydrogen Sulfate
Na ⁺	Sodium Ion
OH ⁻	Hydroxide
NO	Nitric Oxide
CO ₂	Carbon Dioxide
HCO ₃ ⁻	Bicarbonate
SO ₄ ²⁻	Sulfate
CO ₃ ²⁻	Carbonate
O ₂	Oxygen
NaOH	Sodium Hydroxide

The chemical components were added as per Table 4.1. These components constitute the species making up the incoming CO₂ streams, potential auxiliary streams, as well as those partaking in the reaction mechanism of the flue gas cleaning process. The ELECNRTL (Electrolyte Non-Random Two-Liquid) base method was chosen for the calculation of physical properties in the methods tab. This base method is used for the modeling of electrolytes, which is crucial for aqueous solutions as in this process. The Henry components and Chemistry ID of the electrolyte calculation options were set to be defined by the global reactions of the system. These were defined in the chemistry tab as a set of specified reactions, as per Table 4.2. Further it was specified that all missing parameters should be estimated.

Table 4.2: Global reactions of the system, as specified in Aspen Plus[®].

Reaction	Type	Stoichiometry
1	Equilibrium	$\text{H}_2\text{O} \rightleftharpoons \text{H}^+ + \text{OH}^-$
2	Equilibrium	$\text{CO}_2 + \text{H}_2\text{O} \rightleftharpoons \text{H}^+ + \text{HCO}_3^-$
3	Equilibrium	$\text{HCO}_3^- \rightleftharpoons \text{H}^+ + \text{CO}_3^{2-}$
4	Equilibrium	$\text{H}_2\text{SO}_4 \rightleftharpoons \text{H}^+ + \text{HSO}_4^-$
5	Equilibrium	$\text{HSO}_4^- \rightleftharpoons \text{H}^+ + \text{SO}_4^{2-}$
6	Equilibrium	$\text{HNO}_3 \rightleftharpoons \text{H}^+ + \text{NO}_3^-$
7	Equilibrium	$\text{O}_2\text{S} + \text{H}_2\text{O} \rightleftharpoons \text{H}^+ + \text{HSO}_3^-$
8	Equilibrium	$\text{HSO}_3^- \rightleftharpoons \text{H}^+ + \text{SO}_3^{2-}$
9	Equilibrium	$\text{HNO}_2 \rightleftharpoons \text{H}^+ + \text{NO}_2^-$
NAOH	Dissociation	$\text{NaOH} \longrightarrow \text{Na}^+ + \text{OH}^-$

4.1.2 Flowsheet and Simulation

A flowsheet of the flue gas cleaning process was constructed in the simulation window of Aspen Plus[®], which was then adapted slightly between cases. The process was based on the adapted sour compression process which has shown promise in earlier studies [37], [9]. An example of a flowsheet used for the simulations is shown in Figure 4.2.

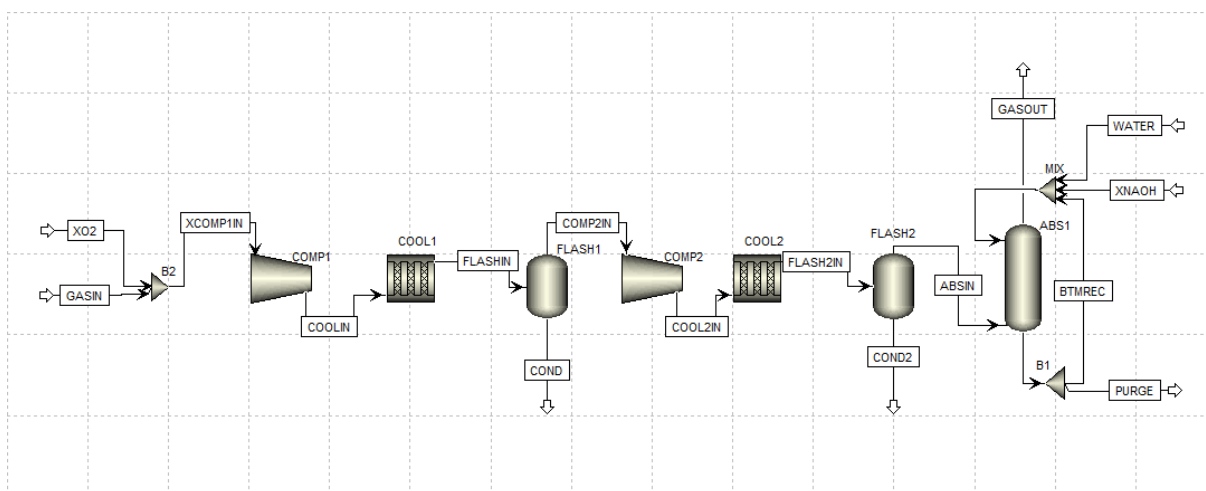


Figure 4.2: Flowsheet of sour compression process in Aspen Plus®.

A compressor was used to raise the pressure of the incoming gas. The isentropic and mechanical efficiencies were assumed to be 1. The desired discharge pressure was 15 bar, which could be set successfully for CLC. For post-combustion and oxyfuel, an error occurred due to a liquid phase forming inside the compressor. Therefore it was changed iteratively to the highest possible pressure before obtaining the error, which was found at 13.1 bar for both cases. The next unit in the process was an intercooler to cool the compressed gas in order to facilitate condensation. The cooler was modeled as a plug flow reactor (RPlug) with the reactor type set to reactor with specified temperature, and with a linear temperature profile between the compressor outlet temperature to 0 °C. Under configuration, it was specified as a multitube reactor with 200 tubes. The tubes were set to a length of 4 meters and a diameter of 20 cm. The gas phase reaction of the system, i.e. the NO oxidation reaction, was added in the reaction folder of the simulation, as per Table 4.3. It was then added to the intercooler under reactions.

Table 4.3: Gas-phase reaction of the system, as specified in Aspen Plus®.

Reaction	Type	Stoichiometry
1	Kinetic	$2\text{NO} + \text{O}_2 \longrightarrow 2\text{NO}_2$ (MIXED)

After cooling, the gas was flashed to condense water, facilitating further compression. The flash drum (Flash2) was set to be defined by pressure and temperature. The pressure was set to the same value as the discharge pressure from the compressor, and the temperature was lowered incrementally until a liquid water phase was formed in the flash drum. Another compressor was then used to raise the pressure to 30 bar, which is the intended operational pressure of the

sour compression process [9]. After this compression, a second cooler and flash were added according to the same principles as after the first compression. The gas was then led to an absorption column (RadFrac). Under configuration, the calculation type was set to rate-based, as this is the setting used for mass-transfer dependent processes, such as the absorption in this column. The proposed reaction mechanism for the combined NO_x and SO_x cleaning was specified in the reactions folder as per Table 4.4, and subsequently added to all stages of the column. The number of stages was approximated to 20, and both reboiler and condenser were removed.

Table 4.4: Proposed reaction mechanism for combined NO_x and SO_x removal [9].

Reaction	Type	Stoichiometry
1	Kinetic	$2\text{NO}_2 + \text{H}_2\text{O} \longrightarrow \text{HNO}_2 + \text{NO}_3^- + \text{H}^+$
2	Equilibrium	$\text{O}_2\text{S} + \text{H}_2\text{O} \rightleftharpoons \text{HSO}_3^- + \text{H}^+$
3	Equilibrium	$\text{HNO}_2 \rightleftharpoons \text{NO}_2^- + \text{H}^+$
4	Equilibrium	$\text{HSO}_3^- \rightleftharpoons \text{SO}_3^{2-} + \text{H}^+$
5	Equilibrium	$\text{H}_2\text{O} \rightleftharpoons \text{OH}^- + \text{H}^+$
6	Kinetic	$2\text{NO}_2 + \text{HSO}_3^- + \text{H}_2\text{O} \longrightarrow 2\text{HNO}_2 + \text{HSO}_4^-$
7	Equilibrium	$\text{CO}_2 + \text{H}_2\text{O} \rightleftharpoons \text{HCO}_3^- + \text{H}^+$
8	Equilibrium	$\text{HSO}_4^- \rightleftharpoons \text{SO}_4^{2-} + \text{H}^+$
9	Kinetic	$2\text{NO} + \text{O}_2 \longrightarrow 2\text{NO}_2$

Table 4.5: Absorption column internals settings.

Start stage	1
End stage	20
Mode	Rating
Internal type	Packed
Packing type	SUPER_RING
Vendor	Rashig
Material	Plastic
Dimension	NO-0.6
Section packed height	varied
Diameter (m)	varied

The column internals were specified according to Table 4.5. The column height was varied as it was subjected to a parameter study, as per Section 4.2.2. The diameter was varied so as to achieve 80% approach to flooding, and thus varied depending on case. Under streams, the gas stream was fed to the column on stage 20 (the bottom stage). Water was used as absorbent, and fed to the column above stage 1, i.e. at the top. The gas stream outlet was specified as a vapor stream with outlet at stage 1, and the bottom liquid as a liquid stream with outlet at stage 20. Under pressure, the stage 1 pressure was set to the same value as that of the final compression, i.e. 30 bar. The absorbent water stream was specified to have the same pressure as that in the column (30 bar), and a temperature of 25 °C. The column was designed to operate at a liquid to gas ratio by mass, R , of approximately 10. R was calculated using Equation 4.1, where \dot{L} is the total liquid mass flow and \dot{G} is the total gas mass flow into the column, both in kg/h.

$$R = \dot{L}/\dot{G} \quad (4.1)$$

The water flow into the column consisted of a recirculated flow from the bottom of the column, as well as a make-up water stream. These were merged with a mixer. As the reaction mechanism in Table 4.4 is only valid for a pH range of 6-7 [9], and the production of acidic compounds make for lower pH conditions, a NaOH stream for pH adjustment was added to this mixer as well. The stream consisted of 1:1 mass ratio of NaOH and water, fed at 25 °C and 30 bar. The absorption process was designed for around pH 6.1, and the NaOH flow was set accordingly. This is because carbonates (HCO_3^- and CO_3^{2-}) are significantly less soluble at lower pH levels. The accumulation of carbonates in the liquid phase is not desired due to precipitation concerns, lowered CO_2 removal efficiency, and higher make-up water consumption, among other things. To prevent said accumulation, a purge stream was added by splitting the bottoms stream, with one end being bled out of the system and the other being recycled and combined with the make-up water. The column was designed to operate at either a concentration of S(VI) compounds (and compounds that would form S(VI) at a later stage as per the reaction mechanism in 4.4), $C_{S(VI)}$, of 25 g/l, or of carbonates, $C_{\text{CO}_3^-}$, of around 50 g/l in the purge stream, whichever was found to be limiting first. These limits were set to limit the risk of precipitation. $C_{S(VI)}$ was found using Equation 4.2, where \dot{m} denotes mass flow given in kg/h and \dot{Q} volume flow given in m^3/h . Similarly, $C_{\text{CO}_3^-}$ was found using Equation 4.3. The split fraction of water being returned to the absorber inlet and make-up water flow were varied iteratively until a limiting concentration was reached, while maintaining R around 10.

$$C_{S(VI)} = \frac{\dot{m}_{\text{HSO}_3^-} + \dot{m}_{\text{SO}_3^{2-}} + \dot{m}_{\text{HSO}_4^-} + \dot{m}_{\text{SO}_4^{2-}}}{\dot{Q}_{\text{water}}} \quad (4.2)$$

$$C_{\text{CO}_3^-} = \frac{\dot{m}_{\text{HCO}_3^-} + \dot{m}_{\text{CO}_3^{2-}}}{\dot{Q}_{\text{water}}} \quad (4.3)$$

Table 4.6: Ingoing gas composition, in volume fractions.

Specie	Post-combustion	Oxyfuel	CLC
CO ₂	0.997	0.799	0.92
O ₂	9.25 E-5	0.046	0.01
N ₂	2.47 E-3	0.154	0.02916
NO	2.65 E-5	3.64 E-4	4 E-4
NO ₂	2.94 E-6	4.05 E-5	4 E-5
SO ₂	3.36 E-5	4.25 E-4	4 E-4
H ₂ O	3.70 E-4	5.50 E-4	0.04

The contents of the ingoing CO₂ stream differed depending on the CO₂ capture method investigated. A summary of the contents of the ingoing streams is shown in Table 4.6. These are average values from spans found in literature [38], [9]. Some species found in literature, namely Ar and CO, were neglected in this model as the proposed reaction mechanism does not account for them. These small contents are balanced by N₂. It was verified that the new, higher N₂ content after this approximation was still within the specified span. The literature only specified the NO_x content as a whole, but not for each of the NO_x species. Therefore the ratio of NO to NO₂ was assumed to be 10:1 [9]. The post-combustion gas is characterized by already being a high-purity CO₂ stream with comparatively small concentrations of impurities. The oxyfuel gas still has a high CO₂ content, but N₂ takes up a significant portion. The CLC gas has CO₂ contents somewhere in between post-combustion and oxyfuel. Although similar, there were some minor differences for the models used for the different gas compositions. These, along with other important design parameters, can be seen in Table 4.7.

Table 4.7: Summary of the most important design parameters for the model.

Parameter	Post-comb.	Oxyfuel	CLC
Inlet gas temperature (°C)	57	57	57
Inlet gas pressure (bar)	1	1	1
Inlet gas flow rate (m ³ /h)	15500	15500	15500
Compressor 1 discharge pressure (bar)	13.1	13.1	15
Intercooler 1 inlet temperature (°C)	276.77	291.27	278.83
Number of tubes, intercoolers 1 and 2	200	200	200
Tube length, intercoolers 1 and 2 (m)	4	10	10
Tube diameter, intercoolers 1 and 2 (m)	0.2	0.2	0.2
Outlet temp. intercoolers 1 and 2 (°C)	0	0	0
Flash 1 temperature (°C)	0	0	0
Flash 1 pressure (bar)	13.1	13.1	15
Compressor 2 discharge pressure (bar)	30	30	30
Intercooler 2 inlet temperature (°C)	61.45	61.85	60.62
Flash 2 temperature (°C)	0	0	0
Flash 2 pressure (bar)	30	30	30
Absorption column number of stages	20	20	20
R	9.81	10.14	10.78
pH, column stage 1	6.09	6.16	6.15
pH, column stage 20	6.08	6.12	6.08

4.2 Design Parameter Study

There are several important parameters that impact the effectiveness of this process. To investigate the effect of some of these, a parameter study was conducted.

4.2.1 NO Oxidation

Parameters impacting the rate of oxidation of NO to NO₂ were investigated. The reasoning behind this is that NO is much less soluble in water than NO₂, which makes it desirable to oxidize as much NO as possible for effective NO_x removal. It was investigated whether the presence of

O₂, change in pressure, or change in residence time in the intercoolers had considerable effects. Since this oxidation takes place before the absorption stage itself, the process stages upstream of the absorption column were isolated. The contents of the ingoing gas were normalized to only contain CO₂, NO, NO₂, and in the case of pressure change and residence time, O₂. To investigate the effects of adding O₂, an extra stream was added to the process inlet gas with a mixer instead. The flow of O₂ was raised in increments, and the total percentage of O₂ in the gas was noted. To better understand where the oxidation occurred, the NO content was noted for several steps in the process: before the first and second compressors, before the first and second intercoolers, as well as the inlet to the (now disconnected) absorber. The flash tanks were disregarded as they only separate water, and no oxidation occurs there. When investigating the effects of pressure change, only the second compressor was considered. This because the pressure of the first compressor could not be raised further as a liquid phase formed in the compressor for some capture methods. The discharge pressure of the second compressor was raised in increments of 15 bar, from 15 to 60 bar. The final pressure raise was limited to 73 bar, so as to not achieve supercritical conditions of the CO₂ stream, as the absorption demands a gas phase stream. As the discharge pressure increased, so did the outlet stream temperature. This meant the new value had to be carried over to the temperature interval specification of the intercooler. To investigate the impact of change in residence time in the intercoolers, their tube lengths were varied, as a longer tube takes longer for the gas to flow through. To take the existing temperature profile into account, a second tube reactor was added after the already existing tube reactor used to model the intercooler investigated at that time. This reactor was given a constant temperature which was the same as the outlet of the original intercooler. If modeled only as one reactor, it would result in a less effective intercooler as it would take a much longer length to reach the same outlet temperature. The intention was instead to model an intercooler where NO was allowed a longer time to oxidize at a low temperature, since this is favored. The combined investigated lengths were 1, 4, 10, 100 and 1000 meters. The first tube reactor in the modeled intercooler was kept at the same length as initially, 4 m, except for a tube length of 1 m where it was shortened. The corresponding residence times τ_{tube} were then calculated using Equation 4.4, where l is the tube length in m, Q is the gas volumetric flow rate in m³/s, and d is the diameter in m.

$$\tau_{tube} = \frac{l}{\frac{Q}{200} / \frac{\pi d^2}{4}} \quad (4.4)$$

4.2.2 Absorption Column

Since the combined NO_x and SO_x removal takes place in the absorption column, some parameters pertaining to this unit were investigated. These were column height, pH, and R . This was done for the oxyfuel process, as it had the highest level of NO_2 at the absorber inlet, making the effects more easily visible. As all considered species of both NO_x and SO_x are affected in this step, the contents of all these species were noted for the absorption column gas outlet. To investigate the effects of column height, the section packed height of the column internals was raised in increments of 1 m, from 1 to 10 m. The corresponding gas residence times were then estimated using Equation 4.5, where h is the column height in m and ε is the packing material void fraction, which in this case was 0.925.

$$\tau_{\text{absorber}} = \frac{h\varepsilon}{Q/\frac{\pi d^2}{4}} \quad (4.5)$$

To investigate the impact of pH, the amount of NaOH solution added to the absorber was varied. The upper and lower flow limits were found iteratively by reading the corresponding pH levels at the top and bottom stages, within the range 6-7. Changes in total liquid flow into the column, and by extension R , as a consequence of varying the flow of NaOH solution were compensated by varying the make-up water flow. Finally, R was varied by changing the split fraction of the flow being recirculated back to the absorber inlet.

5

Results

Using the model described in Section 4.1, some resulting values of important parameters were obtained for the different inlet gases. They are summarized in Table 5.1

Table 5.1: Summary of important resulting parameters.

Parameter	Post-comb.	Oxyfuel	CLC
Absorption column height (m)	3	3	3
Absorption column diameter (m)	1.247	1.398	1.377
Scrubbing water flow rate (kg/h)	1600	2000	2000
Recirculation split fraction	0.9925	0.99	0.99
NaOH solution flow rate (L/h)	75	130	130
Absorber inlet S(VI) concentration (g/L)	1.00	10.71	8.19
Absorber inlet CO ₃ concentration (g/L)	48.68	54.54	57.52

As the oxidation of NO to NO₂ is vital for NO_x absorption, the extents of NO oxidation for all gases across the oxidation stage are shown in Table 5.2.

Table 5.2: NO flows and oxidation results for the process models.

	Post-comb.	Oxyfuel	CLC
Inlet NO concentration (ppm dry)	26.5	368	417
NO concentration at absorber inlet (ppm dry)	26.03	2.15	3.54
NO oxidation (%)	1.67	99.40	99.15

As evident from Table 5.2, the post-combustion case struggles to oxidize NO to NO₂, whereas the oxyfuel and CLC cases see significantly higher grades of oxidation, and consequently lower NO concentrations at the absorber inlet. For future analyses of the post-combustion system in this section (Tables 5.3, 5.4, and 5.5), all NO was oxidized manually by entering it as NO₂. This could represent a case where a method other than pressure increase has been used for NO oxidation. The resulting composition of the outgoing gases can be seen in Table 5.3.

Table 5.3: Outgoing gas composition for process models, in mol-ppm unless otherwise specified, with specifications used for reference.

Specie	Post-com.	Oxyfuel	CLC	Spec. Aramis	Spec. N. Lights
CO ₂ (mol%)	99.68	79.18	95.83	≥ 95	≥ 99.81
O ₂	92.91	4.23 (mol%)	1.03 (mol%)	≤ 10	≤ 10
N ₂	2485	15.83 (mol%)	3.06 (mol%)	≤ 2.4 (mol%)	≤ 50
NO	0	3.16	3.37	≤ 1.5 (NO _x)	≤ 1.5 (NO _x)
NO ₂	0.00001	0.01	0.001	≤ 1.5 (NO _x)	≤ 1.5 (NO _x)
SO ₂	0.00007	0.0001	0.0001	≤ 10	≤ 10
H ₂ O	578	2653	792	≤ 30	≤ 30

From Table 5.2, it is clear that the process is ineffective in lowering the NO_x content effectively for post-combustion gas. However with manually oxidized NO, the NO_x and SO_x contents are well within the specifications both for the Aramis transport hub and Northern Lights storage site. This is however with the assumption of full NO oxidation. For oxyfuel and CLC on the other hand, it is clear that the NO_x content has decreased considerably but is still slightly higher than the specifications. This is because a small fraction of NO remains unoxidized. NO₂ and SO₂ have been absorbed almost completely for all cases. Furthermore it is worthy of notice that as there are high concentrations of other components that will need to be removed, the NO_x concentration of the final product will be higher. Most notably for oxyfuel, it is clear that the CO₂ content is much lower than for post-combustion, with N₂ and O₂ taking up significant shares instead. As for N₂, it is clear that there is a significant amount left for all cases. For post-combustion and CLC the level is acceptable for transport in the Aramis hub, but not for storage at the Northern Lights site. However for oxyfuel, the N₂ content is much too high for both. The O₂ content is much lower for post-combustion gas than for oxyfuel and CLC, although still much too high. Finally, high H₂O content is a common issue for all cases.

The contents of the water bled out of the system were also noted. In Table 5.4, species with noteworthy concentrations (>1 mg/L) in the bleed water are gathered.

Table 5.4: Concentration of accumulated species in bleed water (g/L).
* Released upon pressure decrease.

Specie	Post-combustion	Oxyfuel	CLC
N ₂	0.01	0.07	0.01
HNO ₂	0.06	0.39	0.43
NO ₂ ⁻	0.63	4.62	4.60
HSO ₃ ⁻	0.40	5.57	3.00
SO ₄ ²⁻	0.72	5.22	5.24
CO ₂ [*]	32.44	20.93	24.80
HCO ₃ ⁻	47.69	51.05	52.82
CO ₃ ²⁻	0.01	0.03	0.03
Na ⁺	18.75	25.64	25.58

As evident from Table 5.4, there are many species with noteworthy concentrations in the bleed water. For example, a notable amount of CO₂ is present. This means that some CO₂ is lost from the system. The CO₂ loss for each case, as defined by Equation 5.1, is found in Table 5.5.

$$loss = 1 - \dot{m}_{CO_2,in} / \dot{m}_{CO_2,out} \quad (5.1)$$

Table 5.5: CO₂ losses from the system.

	Post-combustion	Oxyfuel	CLC
CO ₂ loss (%)	0.47	0.65	0.66

5.1 Parameter Study

A parameter study of some important process parameters was conducted. This section will present the results of this analysis.

5.1.1 NO Oxidation

The results of the parameter study pertaining to the impact of O_2 concentration on the rate of oxidation are shown in Figure 5.1.

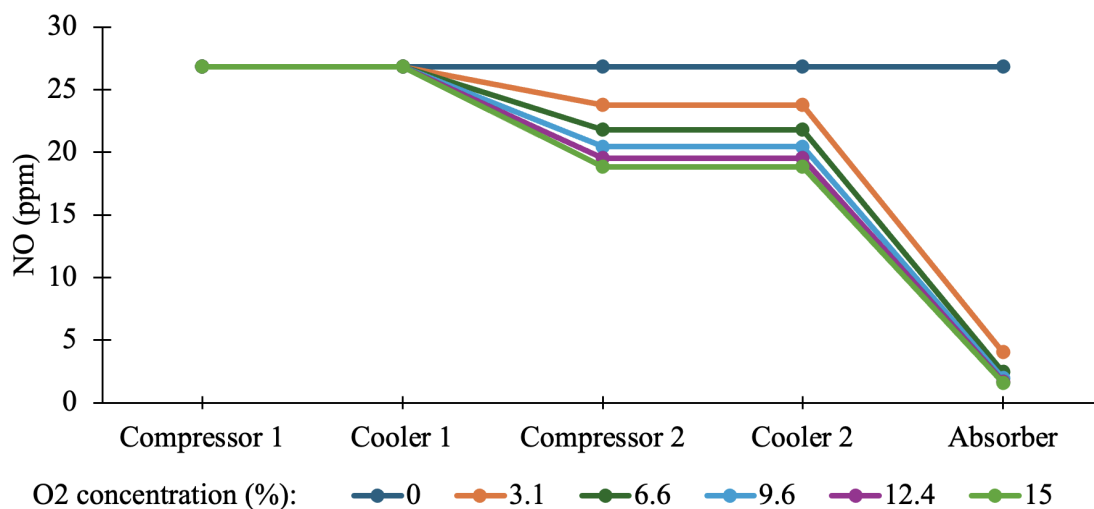


Figure 5.1: Graph of NO content across the process at varying oxygen levels in %, for post-combustion gas.

Evidently, higher O_2 concentrations significantly increase the rate of NO oxidation, as all cases where O_2 was added show a considerably lower NO content going into the absorber. However, the specific amount of oxygen added is not as important, as the difference in NO content is smaller for oxygen concentrations of 3.1% and over. The oxidation occurs in the intercoolers, and the second shows a faster rate of oxidation than the first, judging by the slopes in the graph.

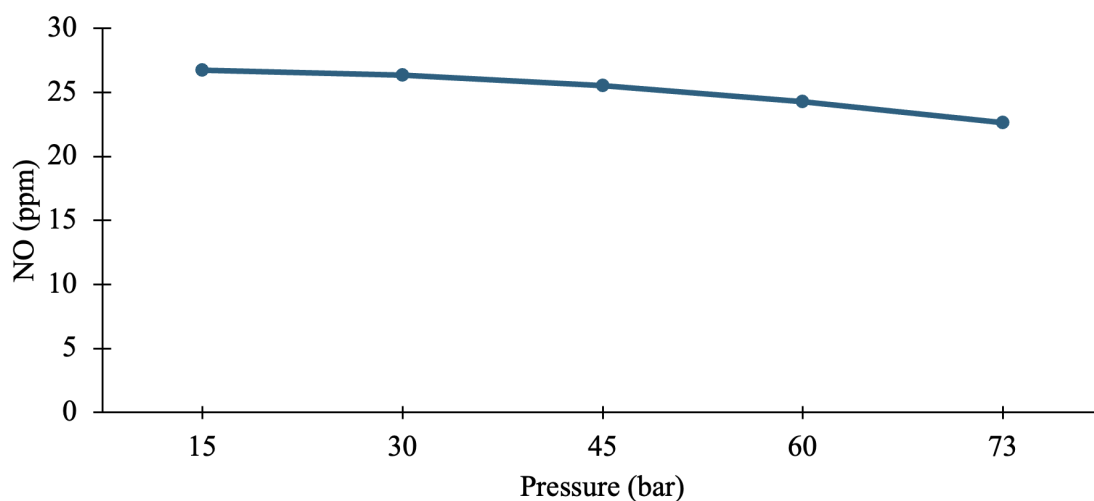


Figure 5.2: Graph of NO content depending on discharge pressure of the second compressor, for post-combustion gas (0.1% O_2).

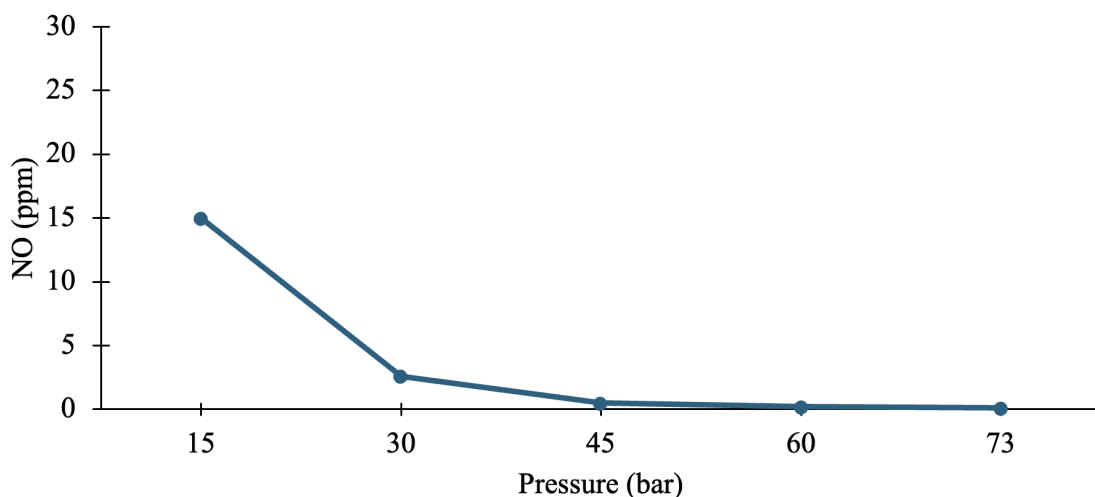


Figure 5.3: Graph of NO content depending on discharge pressure of the second compressor, for oxyfuel gas (5.5% O₂).

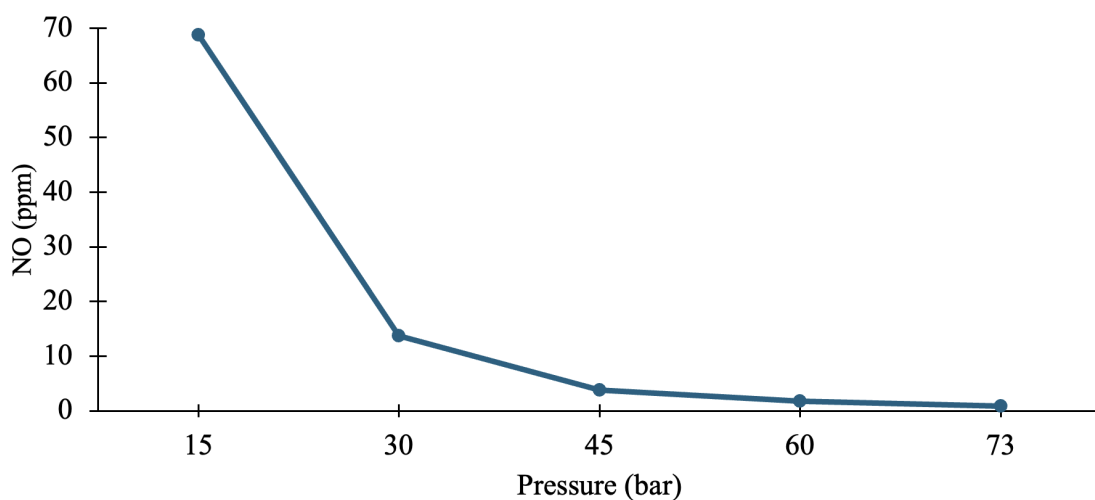


Figure 5.4: Graph of NO content depending on discharge pressure of the second compressor, for CLC gas (1.1% O₂).

Pressure also influences the rate of NO oxidation noticeably, as seen in Figures 5.2, 5.3, and 5.4. The NO content going into the absorber is reduced when discharge pressure of the second compressor is increased. Furthermore, it is apparent that the oxyfuel and CLC gases have a stronger tendency to oxidize NO as the pressure increases, thus making this a more effective method for these gases. The effect of varying the residence times was also investigated. The tested tube lengths and their associated residence times as calculated from Equation 4.4 are shown in Table 5.6. The NO_x oxidation results for the first intercooler are shown in Figures 5.5, 5.6, and 5.7 for the post-combustion, oxyfuel and CLC gases respectively.

Table 5.6: Tube lengths and their corresponding residence times.

Tube length (m)	Residence time (s)
1	1.459
4	5.837
10	14.59
100	149.9
1000	1459

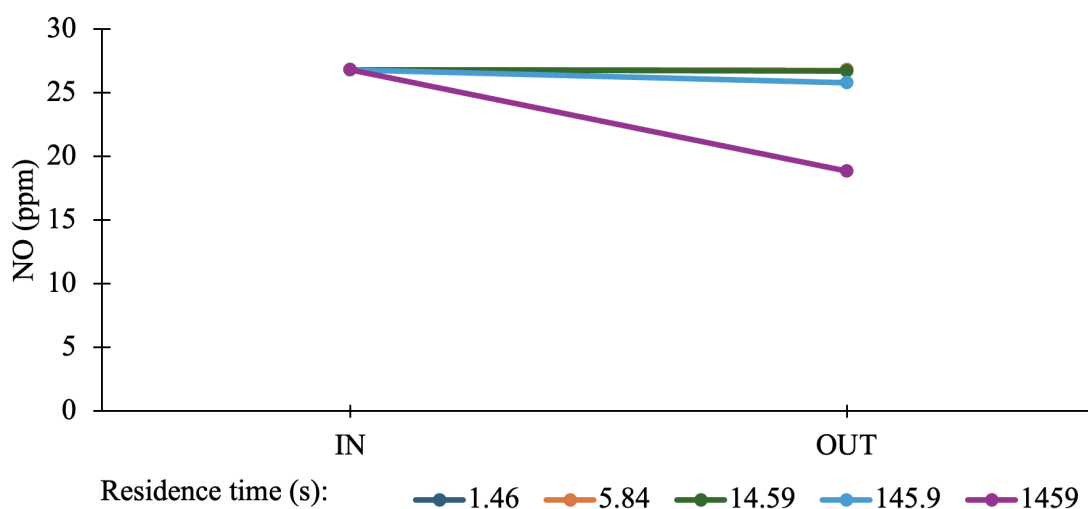


Figure 5.5: Graph of NO content depending on residence time in the first intercooler, for post-combustion gas.

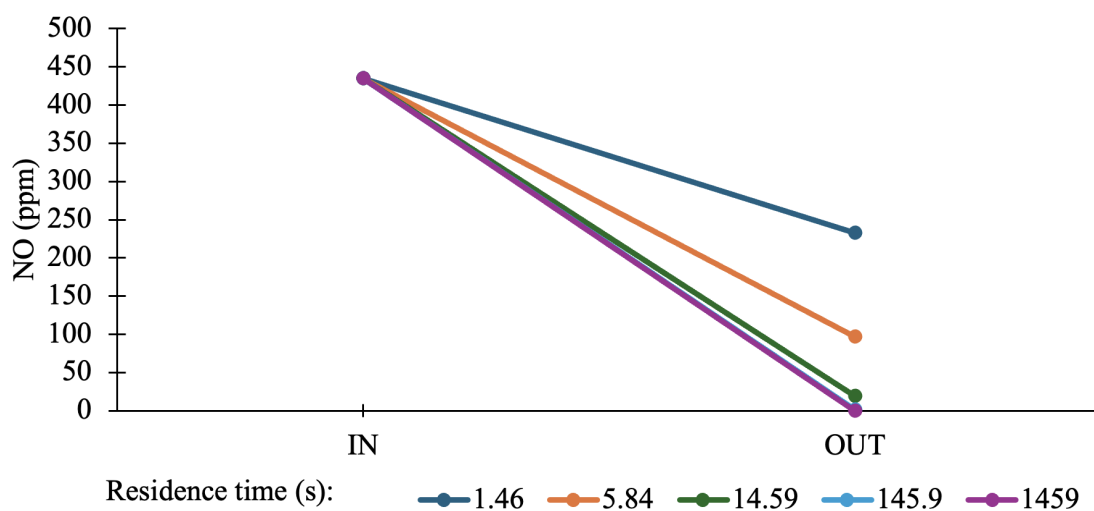


Figure 5.6: Graph of NO content depending on residence time in the first intercooler, for oxyfuel gas.

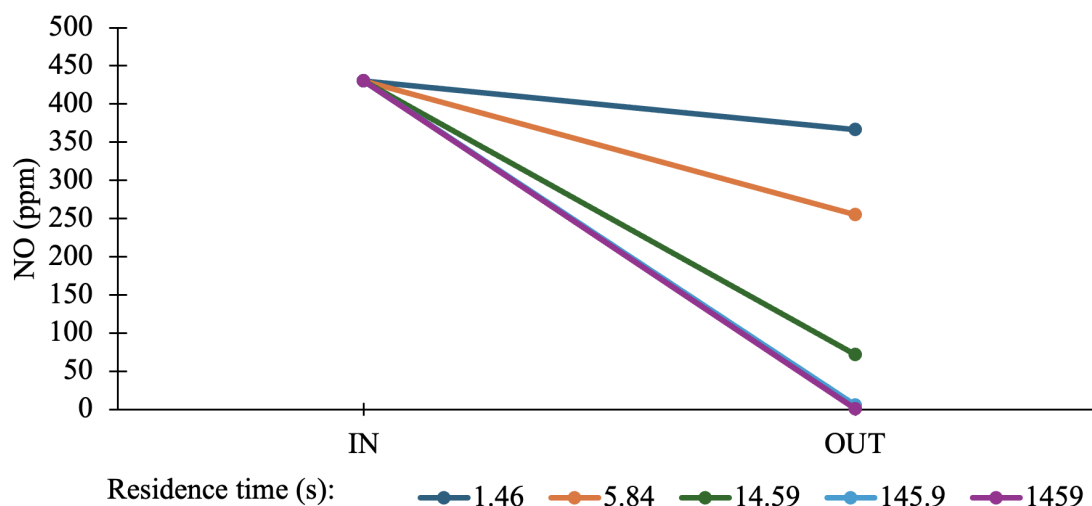


Figure 5.7: Graph of NO content depending on residence time in the first intercooler, for CLC gas.

From Figure 5.5 it is apparent that for post-combustion gas composition, increasing the residence time in the first intercooler is a comparatively ineffective method, even at extreme lengths. The reduction in NO is insignificant with this action alone. However for the other gases, shown in Figures 5.6 and 5.7, the effect is more profound. The results of the same analysis, but for the second intercooler, can be seen in Figures 5.8, 5.9, and 5.10. For all gases, NO oxidizes to a greater extent in the second intercooler compared to the first. It is however worthy of notice that for the post-combustion gas, the impact is only significant for longer residence times. For the other gases, very low NO levels can be reached even for shorter residence times.

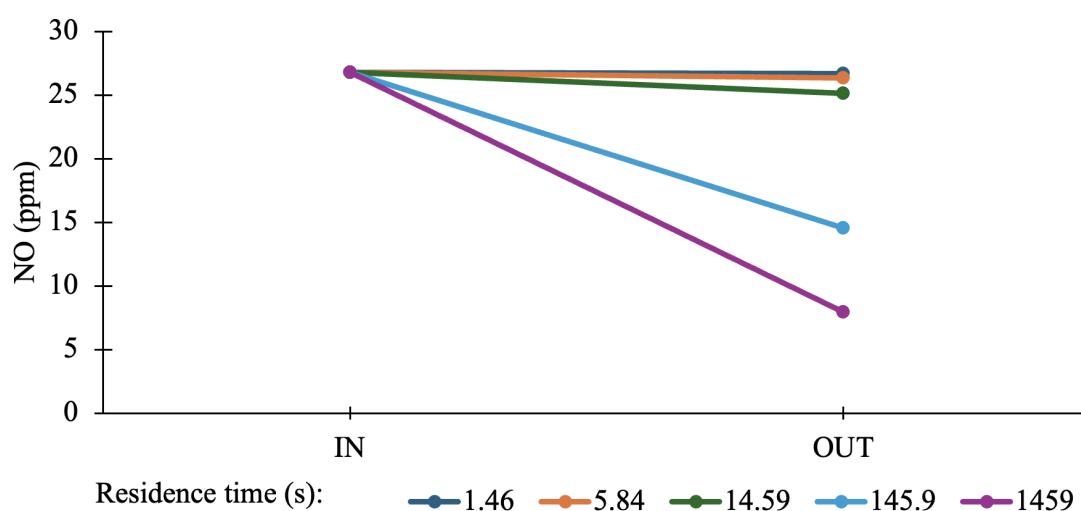


Figure 5.8: Graph of NO content depending on residence time in the second intercooler, for post-combustion gas.

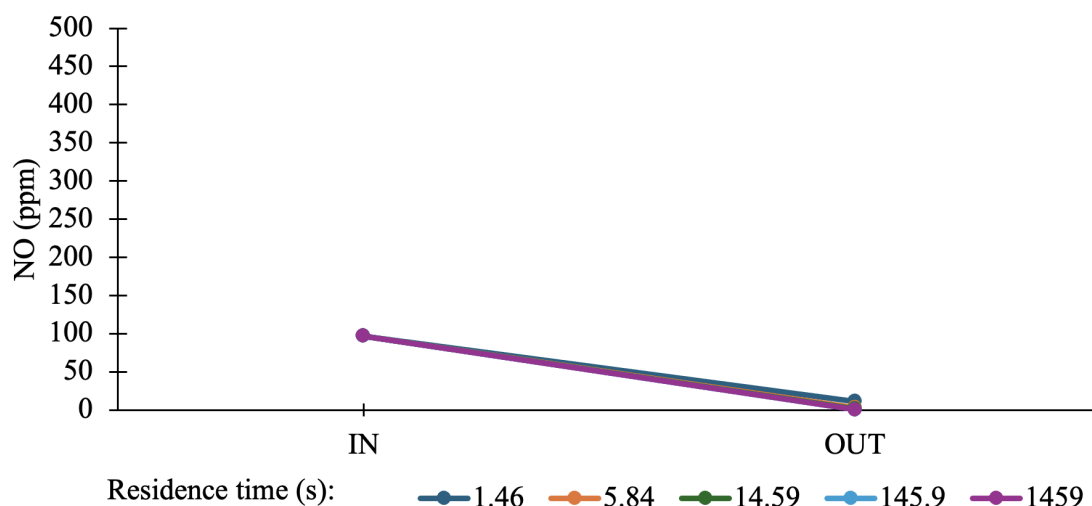


Figure 5.9: Graph of NO content depending on residence time in the second intercooler, for oxyfuel gas.

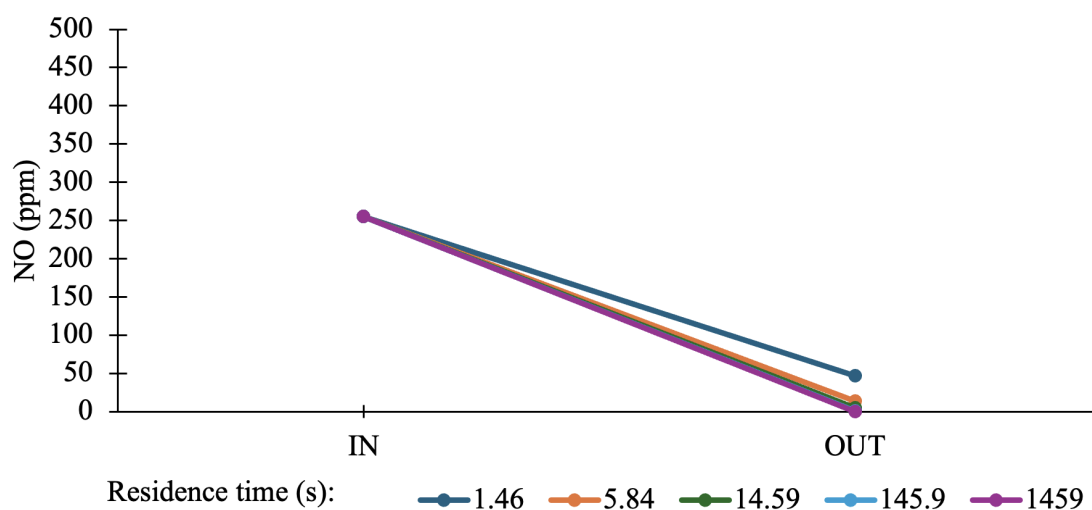


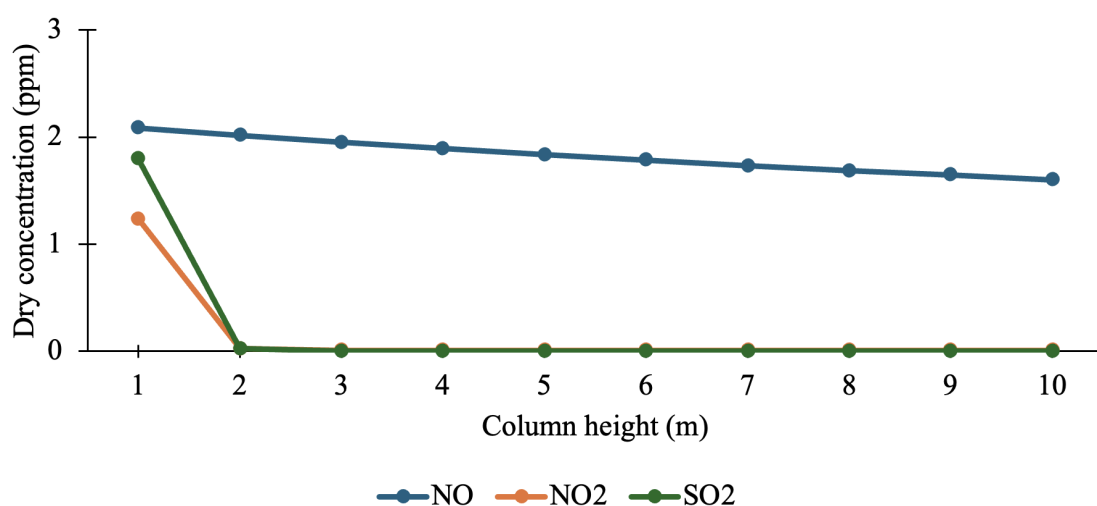
Figure 5.10: Graph of NO content depending on residence time in the second intercooler, for CLC gas.

5.1.2 Absorption Column

The results of the parameter study of the absorption column height can be viewed in Figure 5.11, and the corresponding residence times as estimated from Equation 4.5 in Table 5.7.

Table 5.7: Column heights and their corresponding residence times.

Column height (m)	Residence time (s)
1	11.34
2	22.69
3	34.03
4	45.37
5	56.71
6	68.06
7	79.40
8	90.74
9	102.08
10	113.43

**Figure 5.11:** Graph of NO content depending on column height, for oxyfuel gas.

It is clear that the column height has no drastic effect on the absorption process. The exception is at 1 meter, where the absorption of NO₂ and SO₂ is less effective. At heights of 2 meters and above, NO₂ and SO₂ are removed virtually completely. There is however a slight decrease in NO content at higher column heights, but this effect is not significant. The effects on NO_x and SO_x content due to pH are illustrated in Figure 5.12.

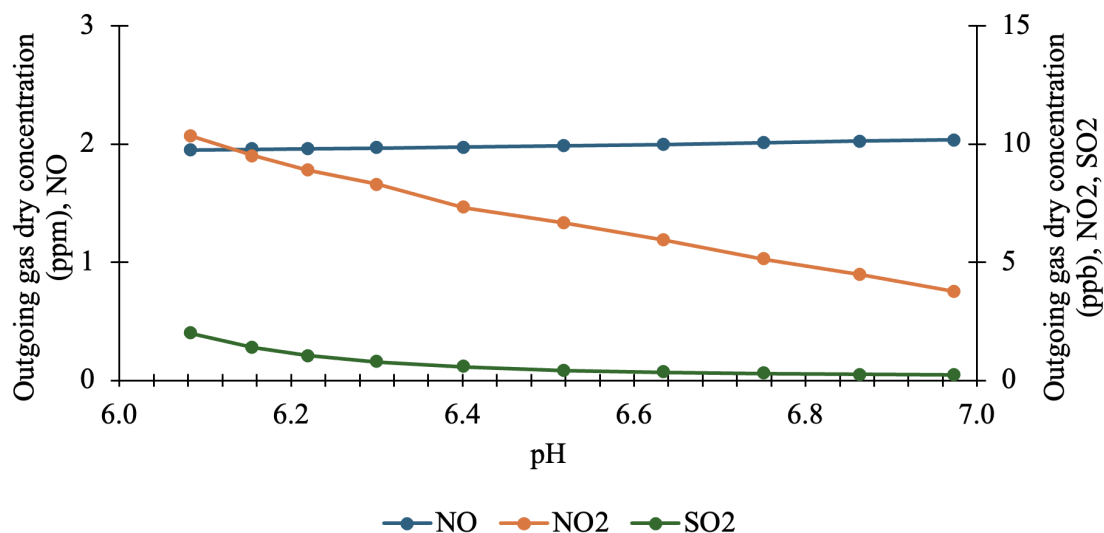


Figure 5.12: Graph of NO content depending on absorber pH, for oxyfuel gas.

It is evident that varying pH has too small of an effect to take into consideration in terms of absorption capabilities. However, the pH has an important relationship to the solubility of carbonates, as made evident from Figure 5.13.

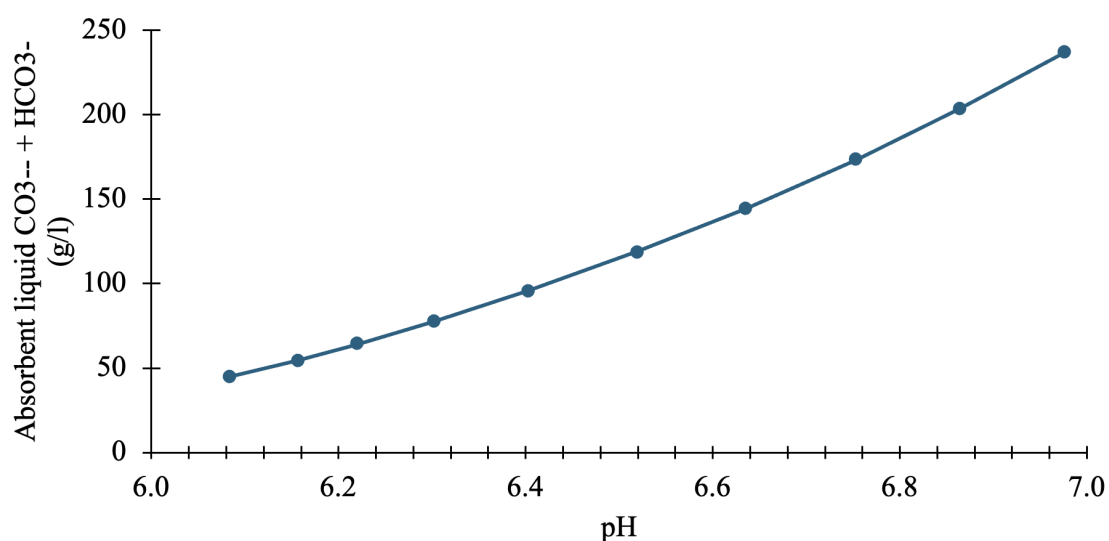


Figure 5.13: Graph of absorbent liquid carbonate content at varying pH, for oxyfuel gas.

Clearly, increasing pH significantly increases the uptake of carbonates in the absorbent liquid stream. As for R , the effects of varying this parameter are shown in Figure 5.14.

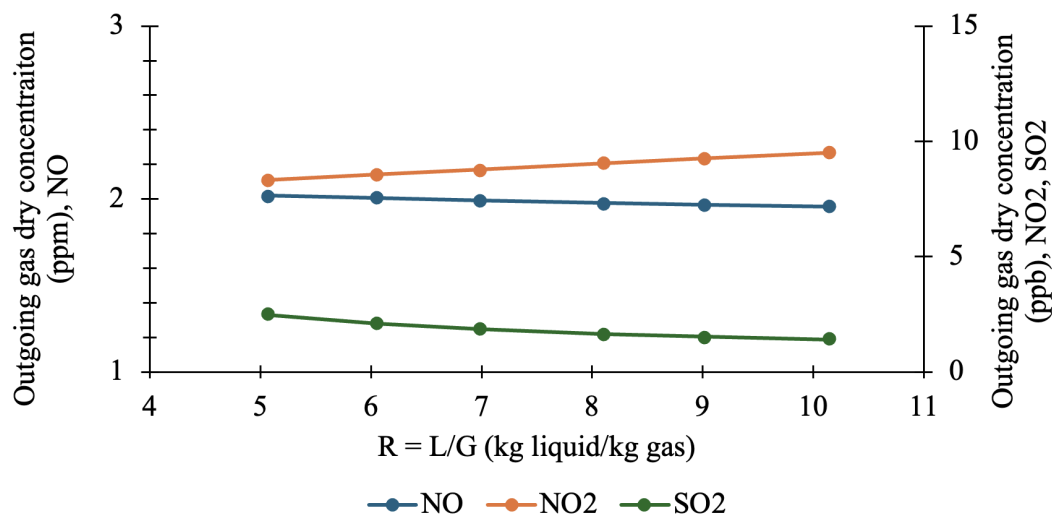


Figure 5.14: Graph of NO content depending on absorber R , for oxyfuel gas.

As for the other parameters, there is no drastic impact on the absorbing qualities when varying R . There is a minuscule decrease in NO concentration at higher R , but this effect is also too small to account for. Here again, as for all investigated parameters pertaining to the absorption column, it is clear that NO_2 and SO_2 are absorbed effectively to almost nonexistent levels irrespective of change in value. Due to the reduced liquid flows at lower R , the absorption column diameter was reduced so as to maintain 80% flooding. The investigated split fractions, resulting values of R , and their corresponding column diameters are shown in Table 5.8.

Table 5.8: Investigated split fractions, resulting R , and associated column diameters.

Split fraction	R	column diameter (m)
0.99	10.138	1.398
0.98875	9.010	1.351
0.9875	8.109	1.311
0.9855	6.989	1.255
0.98325	6.050	1.204
0.98	5.066	1.144

6

Discussion

The outgoing gas compositions from the process are shown in Table 5.3. Based on the low levels of NO_2 and SO_2 , it seems as though the absorption of these species works better than what has been found previously [9]. However the remaining amount of NO in the outgoing gas for oxyfuel and CLC shows that pressurization alone, at least to the degree in which it has been used for this thesis, leaves something to be desired in terms of NO oxidation as the NO_x targets are not quite met due to remaining NO. Furthermore, when analyzing the contents of the bleed water in Table 5.4, high carbonate concentrations are observed. S(IV) and S(VI) concentrations are comparatively insignificant in terms of issues associated with accumulation, but the presence of NO_2^- and SO_4^{2-} shows that the reaction mechanism works as intended. This since these are the desired water soluble species, as per Section 3.3.2. The high Na^+ concentration comes from the addition of NaOH for pH adjustment. While not within the scope of this thesis, this could be an issue depending on what is done with this stream after it has been bled out. For example, there could be limits to consider if this stream were to be released to natural bodies of water or used for other processes. There is also a high concentration of dissolved CO_2 , which is consistent with Henry's law and the high partial pressure of CO_2 in the gas. Once the high pressure is released, so is CO_2 from the liquid stream. As mentioned, this gives a CO_2 loss as per Table 5.5. Although small in terms of percentage, this fraction can add up to large volumes depending on inlet gas flow. This can again be attributed to the higher CO_2 partial pressure, which causes more CO_2 to be dissolved in the water.

6.1 Parameter Study

In this section, the results of the conducted parameter study will be discussed in more detail, and how this affected the model design process.

6.1.1 NO Oxidation

From Figure 5.1 it is clear that O₂ concentration is vital for NO oxidation, as higher O₂ concentrations result in less outgoing NO. This is further confirmed by the results of Table 5.2, which shows that the oxyfuel and CLC cases have dramatically higher extents of oxidation than the post-combustion process. This improvement can be attributed to the higher O₂ contents of these gases, as seen in Table 4.6. Arguably this makes oxyfuel and CLC gases inherently more suited to pressurization as they are more prone to NO oxidation due to the higher oxygen concentration. It would also be possible to use oxidation chemicals to oxidize NO fully or at least sufficiently, which is a method which has worked well under atmospheric conditions [35]. It can be argued that this is counterproductive, as pressurization can be viewed as an alternative method to the use of oxidation chemicals. Although this is partly the case, only smaller amounts of oxidation chemicals would be needed when used as a compliment to raised pressures.

The effect of pressure, visualized in Figures 5.2, 5.3, and 5.4 indicate that higher pressures promote NO oxidization. This is due to the increase in partial pressure of both NO and O₂, accelerating the oxidation to NO₂. This trend strengthens the argument for pressurized processes as a viable alternative to atmospheric processes for NO_x removal, as the desired effect of raising the pressure has been achieved. However, the results found in Figure 5.2 are for the post-combustion process, with very little O₂ content. The effect is increased greatly for the oxyfuel and CLC gases, which is reasonable since these gases entail an even higher partial pressure of oxygen when the pressure is raised, as they are more oxygen-rich.

As for intercooler residence time, it is observable from Figures 5.5 and 5.8 that longer times are beneficial for NO oxidation. This because it allows longer time for the NO oxidation reaction in Equation 4.3, to take place. Arguably, tube lengths longer than 10 meters are impractical from a technical point of view, but the longer lengths (100 and 1000 meters) aid in showing this effect nonetheless since the effect is minimal for shorter lengths for post-combustion gas. For the oxyfuel and CLC gases, satisfactory NO oxidation can be reached with shorter tube lengths which would also make this method viable to use to increase NO oxidation. It was also found that the effect is greater in the second intercooler than the first. This is since the second intercooler is located after the second compressor, and as such is experiencing a higher pressure. As previously stated, higher pressures promote NO oxidation, which entails a greater effect when it is allowed to continue for a longer time.

6.1.2 NO_x and SO_x Absorption

From Figure 5.11, it is observable that the column height has too small an effect to be taken into account as a measure for improving NO_x absorption. Due to material cost concerns, it might be beneficial on a whole to choose a shorter column length, as the penalty in NO_x absorption capability is comparatively insignificant. For this case, a column height of 3 meters seems appropriate with this in mind. Similarly, the pH also has little to no effect on the absorption itself, as per Figure 5.12. Additionally, varying R as per Figure 5.14 shows that increased liquid absorbent flow does not affect the absorption capabilities. However, smaller R comes with the benefit of smaller column diameters as shown in Table 5.8, which in turn makes for lower material costs. Although cost optimization of the suggested process is outside the scope of this thesis, it should be noted that this would be a valid measure as the compromise in absorption capability is virtually nonexistent.

To limit the use of fresh make-up water, the bottom liquid flow was recirculated back to the absorption column inlet to the largest possible extent. As mentioned previously, this fraction of recirculated water could be limited by the accumulation of either S(VI) or carbonates in the absorbent liquid. For all types of inlet gas, carbonates was found to be the limiting concentration before S(VI). Likely this is due to the very high CO₂ contents across all types of investigated inlet gases. This causes the partial pressure of CO₂ to be very high, in turn causing more HCO₃⁻ to form through reaction 2 in Table 4.2. This is usually not the case, since more conventional flue gases generally contain lower concentrations of CO₂, and are treated at lower pressures. This is an important phenomenon, as carbonate accumulation is commonly not an issue at atmospheric pressures [35]. Since the bleed water is fed out of the system, it can be assumed that the pressure will be released eventually. This shifts the reaction equilibrium back towards the formation of CO₂, releasing it from the bleed water. Either this CO₂ is lost, lessening the effectiveness of the process as a whole, or extra steps need to be taken to ensure its capture. This is also true for dissolved CO₂. From Equations 3.4a-3.4b, one can observe the equilibrium reactions in which the carbonate species are formed. As evident from Figure 5.13, carbonates are significantly more soluble at higher pH. This phenomenon can be explained by the fact that as pH is raised, the concentration of H⁺ decreases. In accordance with Le Chatelier's principle, the equilibria of the the reactions are shifted to replace H⁺, forming carbonates.

6.2 Aftertreatment of Outgoing Gas

Despite this thesis only concerning NO_x and SO_x removal, there are several other contaminants present in the gases that will need to be removed as well. These include N_2 and H_2O , and excess O_2 as per the initial resulting gas compositions in Table 5.3. These species will also need to be removed from the gas so as to be within the specified tolerances, which would concentrate the leftover impurities further. More specifically, this process does not remove O_2 , N_2 , or H_2O , all of which are outside of tolerance for the quality specifications used for reference in Table 3.1.

6.3 Areas of Uncertainty

There are some notable factors that could have had impact on the results presented in this thesis. They will be discussed in more detail in this section.

6.3.1 Pressurized Absorption Processes

The intention of using flue gas cleaning processes at elevated pressures is primarily to use pressure as a means of NO oxidation. Since the CO_2 stream will need to be compressed anyway before being stored, there is also the added benefit of this already being partially done after being subjected to this type of treatment. This however brings some uncertainty regarding the pressurization of the absorption part of the process, as pressurized absorption processes are mostly uncharted territory. The exact effects of pressure on for example mass transfer characteristics and thermodynamics in the context of absorption processes are relatively unknown [39]. The modeling results regarding absorption efficiency are dramatic, as NO_2 and SO_2 are absorbed all but completely while previous experiments at atmospheric pressure achieve around 90% and 99% absorption respectively in this regard [35]. The modeling results thus suggest that elevated pressures impacts the absorption process in a positive way. However one would need to consider the added material costs and potential safety concerns associated with elevated design pressures. Moreover, the calculated residence times in the absorption column from Table 4.5 are only estimated as one would for a column at atmospheric pressure, as it is unknown how to do so accurately for a pressurized absorption column.

6.3.2 Validity of Chemical Model

The reaction mechanism upon which this thesis is based is a suggested mechanism from previous studies. This is an intricate mechanism with several reaction pathways across different pH domains [9]. This model however only accounts for one pH range (6-7), with its associated reaction mechanism. There are other absorption reaction pathways for other domains, which might interfere with the studied mechanism towards the limits of the range 6-7, especially considering the process model in this thesis was run at pH levels towards the lower end of that range. Moreover, for computational purposes, only the reduced reaction mechanism was used in this model. Although this reduced mechanism is comprised of the rate-limiting reactions as determined experimentally [9], there might have been minor improvements in accuracy if the full reaction mechanism were used instead. There is also some uncertainty regarding sulfite oxidation as it is described by the reaction mechanism. The reaction kinetics as they are formulated cannot describe the sulfite oxidation in the way it is observed [35]. Since the co-removal reaction mechanism is reliant on this oxidation, it would be valuable to understand it fully.

6.4 Areas of Further Study

The results in this thesis indicate that pressurized co-removal of NO_x and SO_x is a promising technology, especially with regards to the absorption stage of the process. Consequentially, further studies in this field are encouraged, and some specific areas of study are suggested in this section.

6.4.1 Experimental Trials

Due to this model suggesting the possibility of NO_2 and SO_2 being absorbed to very low levels at high pressures, it would be of interest to investigate if these results can be replicated experimentally. It is possible that there are effects of pressurization that are not accounted for in the model which would have an effect in practice. By extension, it would be beneficial to understand pressurized absorption processes in greater detail. More specifically, the impact of elevated pressures on the underlying mass transfer and thermodynamic phenomena governing absorption could be further studied.

6.4.2 Study of Impact of Sulfur Content

Due to time constraints, simulations on CO₂ streams where bio-based fuels were used for combustion were not conducted. These fuels are, among other things, characterized by lower or nonexistent sulfur contents, in turn giving lower SO_x contents in the exhaust gas. According to the proposed reaction mechanism in Table 4.4, as well as previous studies [35], SO₂ is an integral specie in order for NO₂ to be removed effectively as it forms S(IV) in the absorbent water which facilitates NO₂ removal reactions. However, results from unfinished models point towards NO₂ being effectively removed even with very low S(IV) concentrations in the absorbent water. It would be of interest to model such a process to completion to study the importance of SO₂ presence at higher pressures. If still pointing to the conclusion that the presence of SO₂ is of lesser importance, it would be of interest to conduct a more thorough study of how pressure affects the individual reactions of the reaction mechanism.

6.4.3 Modeling of Alternative Process Configurations

The investigated sour compression process is one of several suggested process configurations for the purpose of pressurized co-removal of NO_x and SO_x [9]. It would certainly be interesting to model other process configurations as well, and compare the results with those from the sour compression process modeled for this thesis.

6.4.4 Process Optimization and Economic Analysis

This thesis has only served to investigate the general possibilities of designing a sour compression process capable of removing NO_x and SO_x to sufficiently low levels, which has resulted in a model that has been quite arbitrarily designed. The process has not been optimized or analyzed in terms of cost, which of course is very relevant for real-world application. For this process, it is valid to question the viability of the likely high initial costs associated with design pressures of this caliber, as well as operational costs of the pressurization in itself. The process can also be optimized in terms of CO₂ loss, since it is of interest to keep as much CO₂ within the system as possible. One example of such an action could be to flash the bleed water stream so that the CO₂ in solution is released, and then return it to the inlet of the first compressor.

7

Conclusion

In this thesis, a numerical model of a sour compression process is constructed and applied to investigate the possibility to meet a selection of CO₂ quality specifications for CO₂ transport and storage. The main conclusion is that the use of pressurized absorption processes, such as the sour compression process, is a promising method for the co-removal of NO_x and SO_x from captured CO₂ streams.

The high pressure accelerates the oxidation of NO to NO₂ in the presence of O₂, which is vital since NO₂ is much more water soluble than NO. Yet, the NO oxidation is the bottleneck of the process and oxidation chemicals may be required to meet stringent CO₂ quality specifications.

Also, pressurized absorption processes show superior efficiency in the absorption of NO₂ and SO₂ relative to atmospheric processes, according to simulation results. The effect of pressure was higher than expected and merits further investigation since little is known about pressurized absorption in general.

Moreover, it can be concluded that accumulation of carbonates is an issue during pressurized absorption, in contrast to atmospheric processes. This is since a higher partial pressure of CO₂ causes more CO₂ to be dissolved in the water. The carbonate concentration is strongly related to pH. Because of these factors, there is a noteworthy CO₂ loss from the system.

If pressurized processes are optimized and the underlying phenomena behind pressurized absorption are better understood, it is possible that this can be a viable method for effective NO_x and SO_x removal in the future.

Bibliography

1. Gars J and Olovsson C. Fuel for economic growth? *Journal of Economic Theory* 2019; 184:104941. DOI: <https://doi.org/10.1016/j.jet.2019.104941>. Available from: <https://www.sciencedirect.com/science/article/pii/S002205311930095X>
2. Yang X. Is fossil fuel intensity adversely affecting health improvement and sustainability? *Resources Policy* 2025; 101:105388. DOI: <https://doi.org/10.1016/j.resourpol.2024.105388>. Available from: <https://www.sciencedirect.com/science/article/pii/S0301420724007554>
3. Chen X, Rahaman MA, Murshed M, Mahmood M, and Hossain AM. Causality analysis of the impacts of petroleum use, economic growth, and technological innovation on carbon emissions in Bangladesh. *Energy* 2023; 267:126565. DOI: <https://doi.org/10.1016/j.energy.2022.126565>. Available from: <https://www.sciencedirect.com/science/article/pii/S0360544222034521>
4. United Nations. Goal 13: Take urgent action to combat climate change and its impacts. 2024. Available from: <https://www.un.org/sustainabledevelopment/climate-change/> [Accessed on: 2025 Apr 28]
5. European Commission. The European Green Deal. 2025. Available from: https://commission.europa.eu/strategy-and-policy/priorities-2019-2024/european-green-deal_en [Accessed on: 2025 Jan 20]
6. Naturvårdsverket. Sveriges klimatmål och klimatpolitiska ramverk. 2025. Available from: <https://www.naturvardsverket.se/amnesomraden/klimatomstallningen/sveriges-klimatarbete/sveriges-klimatmal-och-klimatpolitiska-ramverk/> [Accessed on: 2025 Jan 20]

7. Intergovernmental Panel on Climate Change (IPCC). Climate Change 2023: Synthesis Report. Contribution of Working Groups I, II and III to the Sixth Assessment Report. Ed. by Team CW, Lee H, and Romero J. Geneva, Switzerland: IPCC, 2023 :184. DOI: 10.59327/IPCC/AR6-9789291691647
8. Sonke J, Morland BH, Moulie G, and Franke MS. Corrosion and chemical reactions in impure CO₂. *International Journal of Greenhouse Gas Control* 2024; 133:104075. DOI: <https://doi.org/10.1016/j.ijggc.2024.104075>. Available from: <https://www.sciencedirect.com/science/article/pii/S1750583624000185>
9. Ajdari S. Chemistry and Process Design of Integrated Removal of Nitrogen and Sulfur Oxides in Pressurized Flue Gas Systems. PhD thesis. Gothenburg, Sweden: Chalmers University of Technology, 2019
10. Global CCS Institute. CCS 101: The Basics. 2025. Available from: <https://www.globalccsinstitute.com/resources/ccs-101-the-basics/> [Accessed on: 2025 Jan 23]
11. Luis P. Use of monoethanolamine (MEA) for CO₂ capture in a global scenario: Consequences and alternatives. *Desalination* 2016; 380:93–9. DOI: <https://doi.org/10.1016/j.desal.2015.08.004>. Available from: <https://www.sciencedirect.com/science/article/pii/S001191641500418X>
12. de Meyer F and Jouenne S. Industrial carbon capture by absorption: recent advances and path forward. *Current Opinion in Chemical Engineering* 2022; 38:100868. DOI: <https://doi.org/10.1016/j.coche.2022.100868>. Available from: <https://www.sciencedirect.com/science/article/pii/S2211339822000788>
13. Mathieu P. 9 - Oxyfuel combustion systems and technology for carbon dioxide (CO₂) capture in power plants. *Developments and Innovation in Carbon Dioxide (CO₂) Capture and Storage Technology*. Ed. by Maroto-Valer MM. Vol. 1. Woodhead Publishing Series in Energy. Woodhead Publishing, 2010 :283–319. DOI: <https://doi.org/10.1533/9781845699574.3.283>. Available from: <https://www.sciencedirect.com/science/article/pii/B9781845695330500096>
14. Pröll T. 10 - Fundamentals of chemical looping combustion and introduction to CLC reactor design. *Calcium and Chemical Looping Technology for Power Generation and Carbon Dioxide (CO₂) Capture*. Ed. by Fennell P and Anthony B. Woodhead Publishing

- Series in Energy. Woodhead Publishing, 2015 :197–219. DOI: <https://doi.org/10.1016/B978-0-85709-243-4.00010-0>. Available from: <https://www.sciencedirect.com/science/article/pii/B9780857092434000100>
15. Global CCS Institute. Transporting CO₂. 2018. Available from: https://www.globalccsinstitute.com/wp-content/uploads/2018/12/Global-CCS-Institute-Fact-Sheet_Transporting-CO2-1.pdf [Accessed on: 2025 Feb 4]
 16. Wang H, Chen J, and Li Q. A Review of Pipeline Transportation Technology of Carbon Dioxide. *Proceedings of the IOP Conference Series: Earth and Environmental Science*. Vol. 310. 2019 :032033. DOI: 10.1088/1755-1315/310/3/032033
 17. McKaskle R, Beitler C, Dombrowski K, and Fisher K. The Engineer’s Guide to CO₂ Transportation Options. *Proceedings of the 16th Greenhouse Gas Control Technologies Conference (GHGT-16)*. 2022 Oct. DOI: 10.2139/ssrn.4278858
 18. McLaughlin H et al. Carbon capture utilization and storage in review: Sociotechnical implications for a carbon reliant world. *Renewable and Sustainable Energy Reviews* 2023; 177:113215. DOI: <https://doi.org/10.1016/j.rser.2023.113215>. Available from: <https://www.sciencedirect.com/science/article/pii/S1364032123000710>
 19. Aramis CCS. Aramis CCS Brochure. 2024 Aug. Available from: https://www.aramis-ccs.com/files/Aramis-brochure_aug24_ENG.pdf [Accessed on: 2025 Apr 16]
 20. Statistics Netherlands (CBS). Emissions of greenhouse gases according to IPCC guidelines, quarter. 2024. Available from: <https://www.cbs.nl/en-gb/figures/detail/84979ENG> [Accessed on: 2025 Jun 4]
 21. Aramis CCS. CO₂ Specifications for Aramis Transport Infrastructure. 2023. Available from: <https://www.aramis-ccs.com/news/co2-specifications-for-aramis-transport-infrastructure/> [Accessed on: 2024 Jan 30]
 22. Equinor. Northern Lights – Equinor. 2025. Available from: <https://www.equinor.com/energy/northern-lights> [Accessed on: 2025 Apr 16]
 23. DNV. Northern Lights and DNV collaborate to update the CO quality specifications for carbon transport and storage. 2024. Available from: <https://www.dnv.com/article/northern-lights-and-dnv-collaborate-to-update-the-co2-quality-specifications-for-carbon-transport-and-storage/> [Accessed on: 2025 Apr 16]

24. Norwegian Environment Agency, Statistics Norway, and Norwegian Institute of Bioeconomy Research. Greenhouse Gas Emissions 1990–2023: National Inventory Document. Tech. rep. M-2948. Oslo, Norway: Norwegian Environment Agency, 2025. Available from: <https://www.miljodirektoratet.no/globalassets/publikasjoner/M2948/M2948.pdf> [Accessed on: 2025 Jun 5]
25. Northern Lights. Liquid CO₂ (LCO₂) Quality Specifications. 2024. Available from: <https://norlights.com/wp-content/uploads/2024/06/NorthernLights-GS-co2-spec2024.pdf> [Accessed on: 2025 Mar 17]
26. Hanson E, Nwakile C, and Hammed VO. Carbon capture, utilization, and storage (CCUS) technologies: Evaluating the effectiveness of advanced CCUS solutions for reducing CO₂ emissions. *Results in Surfaces and Interfaces* 2025; 18:100381. DOI: <https://doi.org/10.1016/j.rsurfi.2024.100381>. Available from: <https://www.sciencedirect.com/science/article/pii/S2666845924002010>
27. Hayat MA, Alhadhrami K, and Elshurafa AM. Which bioenergy with carbon capture and storage (BECCS) pathways can provide net-negative emissions? *International Journal of Greenhouse Gas Control* 2024; 135:104164. DOI: <https://doi.org/10.1016/j.ijggc.2024.104164>. Available from: <https://www.sciencedirect.com/science/article/pii/S1750583624001075>
28. Intergovernmental Panel on Climate Change (IPCC). IPCC Special Report on Global Warming of 1.5 °C — Graphics. 2018. Available from: <https://www.ipcc.ch/sr15/graphics/> [Accessed on: 2025 Apr 16]
29. Morland BH, Dugstad A, Tjelta M, and Svenningsen G. Formation of Strong Acids in Dense Phase CO₂. Vol. All Days. *NACE CORROSION*. 2018 Apr :NACE-2018–11429
30. Morland BH, Tjelta M, Norby T, and Svenningsen G. Acid reactions in hub systems consisting of separate non-reactive CO₂ transport lines. *International Journal of Greenhouse Gas Control* 2019; 87:246–55. DOI: <https://doi.org/10.1016/j.ijggc.2019.05.017>. Available from: <https://www.sciencedirect.com/science/article/pii/S1750583618305899>
31. Morland BH, Dugstad A, and Svenningsen G. Experimental based CO₂ transport specification ensuring material integrity. *International Journal of Greenhouse Gas Control* 2022; 119:103697. DOI: <https://doi.org/10.1016/j.ijggc.2022.103697>. Available

- from: <https://www.sciencedirect.com/science/article/pii/S1750583622001153>
32. Yevtushenko O, Bettge D, Bäßler R, and Bohraus S. Corrosion of CO₂ transport and injection pipeline steels due to the condensation effects caused by SO₂ and NO₂ impurities. *Materials and Corrosion* 2015; 66:334–41. DOI: <https://doi.org/10.1002/maco.201307368>. Available from: <https://onlinelibrary.wiley.com/doi/abs/10.1002/maco.201307368>
 33. Fostås B et al. Effects of NO_x in the flue gas degradation of MEA. *Energy Procedia* 2011; 4. 10th International Conference on Greenhouse Gas Control Technologies:1566–73. DOI: <https://doi.org/10.1016/j.egypro.2011.02.026>. Available from: <https://www.sciencedirect.com/science/article/pii/S1876610211002232>
 34. U.S. Environmental Protection Agency. NO_x: How Nitrogen Oxides Affect the Way We Live and Breathe. 1998. Available from: <https://www3.epa.gov/ttn/catc1/dir1/fnoxdoc.pdf> [Accessed on: 2024 Jan 29]
 35. Johansson J. Absorption Based Systems for Co-removal of Nitrogen Oxides and Sulfur Oxides from Flue Gases. PhD thesis. Gothenburg, Sweden: Chalmers University of Technology, 2022
 36. Henry W and Banks J. III. Experiments on the quantity of gases absorbed by water, at different temperatures, and under different pressures. *Philosophical Transactions of the Royal Society of London* 1803; 93:29–274. DOI: 10.1098/rstl.1803.0004. eprint: <https://royalsocietypublishing.org/doi/pdf/10.1098/rstl.1803.0004>. Available from: <https://royalsocietypublishing.org/doi/abs/10.1098/rstl.1803.0004>
 37. White V, Allam R, and Miller E. Purification of Oxyfuel-Derived CO for Sequestration or EOR. *8th International Conference on Greenhouse Gas Control Technologies (GHGT-8)*. Vol. 1. Trondheim, Norway: Elsevier Science Ltd., 2006 :1–6. Available from: https://www.researchgate.net/profile/Vince-White/publication/237433042_Purification_of_Oxyfuel-Derived_CO2_for_Sequestration_or_EOR/links/02e7e538ebae402de5000000/Purification-of-Oxyfuel-Derived-CO2-for-Sequestration-or-EOR.pdf

38. Porter RTJ et al. Techno-economic assessment of CO₂ quality effect on its storage and transport: CO₂QUEST: An overview of aims, objectives and main findings. *International Journal of Greenhouse Gas Control* 2016; 54:662–81. DOI: <https://doi.org/10.1016/j.ijggc.2016.08.011>. Available from: <https://www.sciencedirect.com/science/article/pii/S1750583616304893>
39. Isa F et al. An overview on CO₂ removal via absorption: Effect of elevated pressures in counter-current packed column. *Journal of Natural Gas Science and Engineering* 2016; 33:666–77. DOI: <https://doi.org/10.1016/j.jngse.2016.06.003>. Available from: <https://www.sciencedirect.com/science/article/pii/S1875510016303869>

DEPARTMENT OF SPACE, EARTH AND ENVIRONMENT
CHALMERS UNIVERSITY OF TECHNOLOGY
Gothenburg, Sweden
www.chalmers.se



CHALMERS
UNIVERSITY OF TECHNOLOGY